



GRADUATE SCHOOL  
EAST TENNESSEE STATE UNIVERSITY

East Tennessee State University  
Digital Commons @ East  
Tennessee State University

---

Electronic Theses and Dissertations

Student Works

---

8-2023

## A Low Cost, Compact Electrochemical Analyzer based on an Open-Source Microcontroller

Michael Kofi Darko Addo  
*East Tennessee State University*

Follow this and additional works at: <https://dc.etsu.edu/etd>

 Part of the [Analytical Chemistry Commons](#)

---

### Recommended Citation

Addo, Michael Kofi Darko, "A Low Cost, Compact Electrochemical Analyzer based on an Open-Source Microcontroller" (2023). *Electronic Theses and Dissertations*. Paper 4258. <https://dc.etsu.edu/etd/4258>

This Thesis - embargo is brought to you for free and open access by the Student Works at Digital Commons @ East Tennessee State University. It has been accepted for inclusion in Electronic Theses and Dissertations by an authorized administrator of Digital Commons @ East Tennessee State University. For more information, please contact [digilib@etsu.edu](mailto:digilib@etsu.edu).

A Low Cost, Compact Electrochemical Analyzer based on an Open-Source Microcontroller

---

A thesis

presented to

the faculty of the Department of Chemistry

East Tennessee State University

In partial fulfillment

of the requirements for the degree

Master of Science in Chemistry

---

by

Michael Kofi Darko Addo

August 2023

---

Gregory W. Bishop, Ph.D., Chair

Catherine E. McCusker, Ph.D.

Dane W. Scott, Ph.D.

Keywords: open-source, potentiostat, microcontroller, pulse-width modulation, pencil graphite

electrode

## ABSTRACT

A Low Cost, Compact Electrochemical Analyzer based on an Open-Source Microcontroller

by

Michael Kofi Darko Addo

Compared to other instruments for chemical analyses, electrochemical analyzers are relatively simple, inexpensive, easy to miniaturize and require little-to-no maintenance. However, like all commercially available instruments, commercial electrochemical analyzers like potentiostats primarily operate as black boxes with manufacturers providing little or no information about internal circuitry and programming. This practice can limit a researcher's ability to develop new techniques or adapt an instrument for applications outside its typical use. In contrast, creators of open-source instruments release all the necessary information for reproduction of the hardware and software – minimizing such barriers to innovation in chemical analyses. Here, we report a low-cost, compact potentiostat based on an open-source Arduino microcontroller capable of performing electrochemical analyses such as cyclic and linear sweep voltammetry with an operating range of  $\pm 208 \mu\text{A}$  and  $\pm 2.5 \text{ V}$ . Performance of the potentiostat is investigated with low-cost pencil graphite electrodes and compared to a commercial potentiostat.

Copyright 2023 by Michael Kofi Darko Addo

All Rights Reserved

## DEDICATION

I dedicate this work to my parents – Mr. Samuel Addo and Mrs. Ruth Addo, my siblings and friends who motivated me to give my best throughout my course of study.

## ACKNOWLEDGMENTS

My profound gratitude to my research advisor, Dr. Gregory W. Bishop for his patience, inspiration, and professional mentorship throughout this project. I would also like to acknowledge Anna E. Curtis for her support and assistance in this project. Lastly, I thank my fellow lab mates Sandra Ehigiator and Yakubu Mohammed for their encouragement.

## TABLE OF CONTENTS

ABSTRACT .....	2
DEDICATION .....	4
ACKNOWLEDGMENTS .....	5
LIST OF TABLES .....	8
LIST OF FIGURES .....	9
LIST OF ABBREVIATIONS.....	10
CHAPTER 1. INTRODUCTION.....	11
Open-Source Instruments .....	11
General Design and Operating Principles of Potentiostats .....	13
Open-Source Potentiostats .....	15
Research Aims.....	24
CHAPTER 2. EXPERIMENTAL.....	26
Materials.....	26
Pencil Graphite Electrode Fabrication .....	26
Electrochemical Characterization .....	28
CHAPTER 3. RESULTS AND DISCUSSION.....	30
Hardware Development of Home-built Potentiostats .....	30
Software Development.....	35
Current-Voltage Measurements with Commercial and Home-built Instruments .....	38
Resistor Tests .....	38
Electrochemical Characterization of Commercial and Home-built Instruments .....	41
CHAPTER 4. CONCLUSIONS AND FUTURE WORK.....	46

REFERENCES .....	48
APPENDICES .....	52
Appendix A: Arduino Sketch for PWM Potentiostat.....	52
Appendix B: Arduino Sketch for External DAC .....	56
VITA.....	60

## LIST OF TABLES

Table 1. Specifications of Some Selected Open-source Potentiostats and their Material Costs (\$USD) at the Time of Publication .....	17
Table 2. Example of Output from a 3-bit Weighted-resistor Ladder DAC .....	20
Table 3. Comparison of Resistor Test Results for Home-built Instruments at 50 mV/s .....	40

## LIST OF FIGURES

Figure 1. An illustrated schematic (simplified circuit diagram) of a simple three-electrode potentiostat.....	14
Figure 2. A digital logic circuit of a 3-bit binary-weighted-input DAC.....	18
Figure 3. An image of an Arduino Uno development board .....	22
Figure 4: Illustration of Pulse Width Modulation (PWM).....	23
Figure 5. Assemble of pencil graphite electrode (PGE) arrays .....	27
Figure 6. Simplified circuit diagram of compact, home-built PWM- and external DAC-based electrochemical analyzers .....	30
Figure 7. Photographs of commercial (CH instruments 760E Electrochemical Workstation) and home-built electrochemical analyzers based on an open-source microcontroller	34
Figure 8. Top-view of components assembled on a breadboard for external DAC-based instrument .....	35
Figure 9. Illustration of DAC/PWM value – time plot.....	36
Figure 10. A flowchart representation of sketch uploaded onto microcontroller.....	37
Figure 11. Linear sweep voltammogram of a 12 k $\Omega$ resistor at 50 mV/s.....	39
Figure 12. Electrochemical response of 10 mM potassium ferricyanide with 0.1 M KCl supporting electrolyte using home-built and commercial instruments with glassy carbon working electrodes.....	42
Figure 13. Electrochemical performances of Home-built and Commercial instruments with pencil graphite electrode.....	44
Figure 14. CV response of pencil graphite electrode before and after Arduino scans .....	45

## LIST OF ABBREVIATIONS

ADC: Analog-To-Digital Converter

ATX: Advanced Technology Extended

CPU: Central Processing Unit

CV: Cyclic Voltammetry

CVC: Current -To-Voltage Converter

DAC: Digital-To-Analog Converter

IDE: Integrated Development Environment

PCB: Printed Circuit Board

PGE: Pencil Graphite Electrode

PWM: Pulse-Width Modulation

USB: Universal Serial Bus

## CHAPTER 1. INTRODUCTION

### *Open-Source Instruments*

Instruments for chemical analyses convert information about the physical or chemical properties of a system under study into data that can be processed and interpreted.<sup>1</sup> While many of the phenomena upon which instrumental methods of analysis are based have been known for over one hundred years, the beginnings of their application for the routine analyses of today can be traced to the inventions of the microprocessor and microcomputer in the 1970s.<sup>1</sup> A microprocessor or central processing unit (CPU) is an integrated circuit capable of performing arithmetic and logic operations, while a microcomputer utilizes one or more CPUs with other circuit components to provide data input and output functions, store data, and enable timing of operations. These advances and continued progress in electronics have resulted in faster, automated data acquisition, increased precision, and accuracy of measurement processes through better control over experimental variables, and wide-spread commercialization of instruments for chemical analysis. However, modern commercial instruments can be expensive and often operate as “black boxes” with limited documentation provided by the manufacturer regarding underlying design and operating principles.<sup>2-4</sup>

The lack of circuit design and programming information can prevent instruments from being applied or interfaced with accessories for measurements outside the manufacturer’s specified use, thereby limiting the potential for innovation and novel applications.<sup>2,3,5</sup> To overcome such limitations imposed by commercial (closed-source) black boxes, the maker and open-source movements, which have already stimulated improvements to accessibility and application of 3D printing technologies,<sup>6,7</sup> have been increasingly applied in recent years to

hardware and software for chemical analyses, resulting in the development of various open-source instruments.<sup>8-14</sup>

Open-source instruments are ones for which design schematics and programming instructions are made available to the public so that others can reproduce or make modifications as permitted by the creator.<sup>5,15-17</sup> However, the quality and accessibility of information provided by a creator about their hardware and software can vary. In some cases, a creator may release the information through self-maintained websites or as supporting information associated with a published article.<sup>5</sup> Oftentimes, creators of open-source instruments share information about their projects on hosting sites like GitHub, Bitbucket, and Gitlab,<sup>18-21</sup> which is preferable as these repositories allow others to view, download, and sometimes contribute freely to the work.<sup>5</sup> Disclosure of critical design and programming aspects of open-source hardware can enable better understanding of instrument performance and limitations as well as the possibility to interface or apply an instrument with other measurement devices and accessories for new applications.<sup>7</sup>

Open-source instruments are increasingly being introduced into classrooms, where they can be utilized to allow students to develop hands-on experience in electronics, coding, and programming. The barrier to these subjects can be lowered even further by developing instruments based on open-source hardware popularized by companies like Arduino, which offer products like open-source microcontroller development boards and harbor online communities of enthusiasts and contributors to share ideas, projects, and code.<sup>22,23</sup> For example, an author reported that graduate students were able to build an open-source wireless potentiometric instrument based on an Arduino Nano microcontroller for pH determination of unknown aqueous solutions.<sup>12</sup> The interactive and immersive environment facilitated by open-source instruments can also help effectively illustrate and demonstrate topics related to principles of signal

generation and data acquisition, which are often limited to coverage based on more generic block and circuit diagrams in traditional classroom settings.<sup>24,25</sup>

While various open-source instruments for chemical analyses including spectrometers and photometers for fluorescence and absorption have been developed for education and research, open-source instruments for electrochemical analyses are among the most widely reported.<sup>26</sup> Electrochemical instruments are particularly well-suited for open-source adaptation due to their relative simplicity, low cost, ease of miniaturization and lack of maintenance. Furthermore, electrochemical techniques like voltammetry and amperometry can exhibit high sensitivity and selectivity, wide linear range, and low limits of detection for many applications. One type of electrochemical analyzer that has seen particular wide-spread use and development in the open-source community over the past decade is the potentiostat. Potentiostats enable control of the potential between two electrodes in an electrochemical cell and measures the resulting current that develops as a result of the applied potential. These instruments are capable of carrying out voltammetric (current as a function of applied potential) and amperometric (current at a particular potential or potentials as a function of time) measurements.<sup>2,3,27-30</sup>

#### *General Design and Operating Principles of Potentiostats*

A potentiostat (Figure 1) controls the potential applied between a reference electrode (RE) and working electrode (WE) while measuring the resulting electrical current generated between the counter electrode (CE) and WE in an electrochemical cell.<sup>2,29,30</sup> At the heart of any potentiostat is a type of small integrated circuit known as an operational amplifier (op amp). An op amp is made up of several transistors (~20) and resistors and operates to output the amplified (on the order of  $10^4$  to  $10^6$  times or more) difference between the two inputs (i.e., noninverting

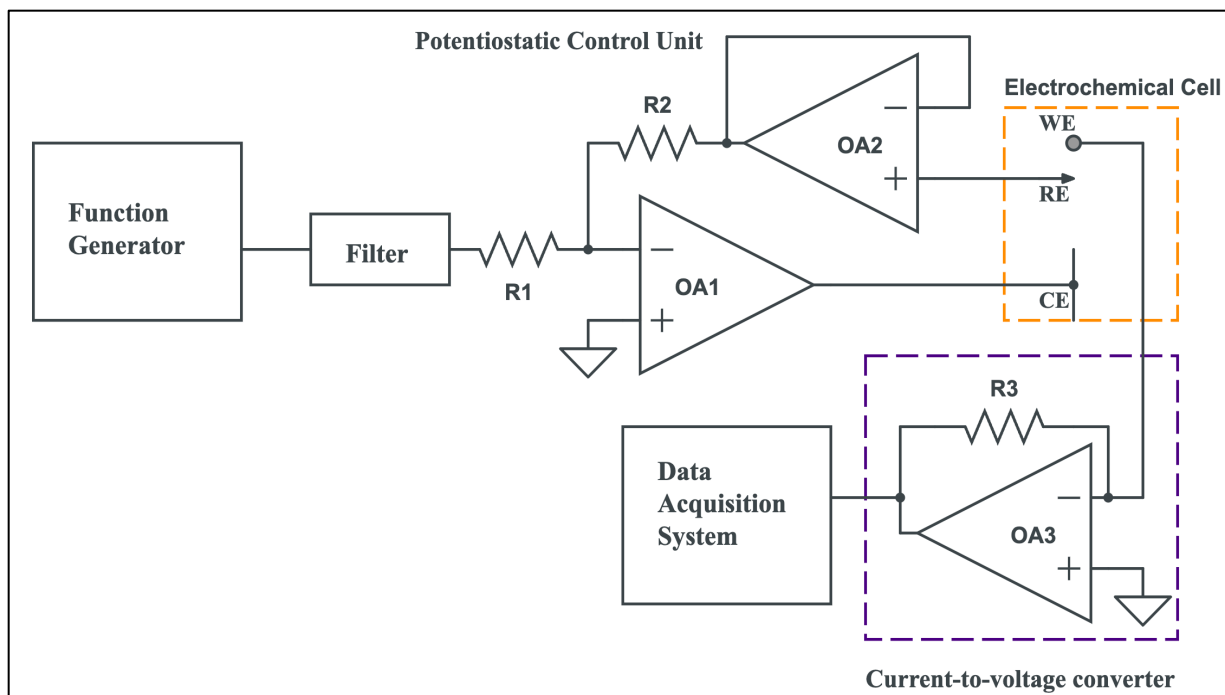


Figure 1. An illustrated schematic (simplified circuit diagram) of a simple three-electrode potentiostat. Operational amplifiers (OA) are labeled. The – and + signs on OAs designate the inverting and noninverting inputs, respectively.

(+) and inverting (-) (Equation 1) without drawing significant current from the source due to the high impedance of the inputs.<sup>1</sup>

$$e_o = A (e_+ - e_-) \quad (1)$$

where  $e_o$  is the output voltage (in V),  $A$  is the open-loop gain,  $e_+$  is the voltage (in V) supplied to the noninverting input, and  $e_-$  is the voltage (in V) supplied to the inverting input.

In a basic potentiostat (Figure 1), an op amp (OA1) acts as a potential control amplifier, controlling the potential of the reference electrode (based on the value  $e_{\text{applied}}$  set by the function generator) with respect to ground. A second op amp (OA2) acts as a voltage follower,<sup>1,31</sup> which is included to ensure that no significant current is drawn from the reference electrode (due to the op amp's high input impedance), while providing an output voltage that is simply the reference

electrode potential  $e_{ref}$ . Due to the high input impedance of OA1, the current at the summing point located near the inverting input of OA1 must add to zero (Equation 2).

$$i_{applied} + i_{ref} = \frac{e_{applied}}{R1} + \frac{e_{ref}}{R2} = 0 \quad (2)$$

If the values of resistors R1 and R2 are equal,  $-e_{ref} = e_{applied}$  vs. ground. Since the working electrode is held at virtual ground by a third op amp (OA3), the working electrode potential  $e_{work}$  (vs.  $e_{ref}$ ) =  $e_{applied}$ .<sup>31</sup> The counter electrode completes the potentiostatic control circuit by providing a point in the system where enough current can be passed in the electrochemical cell to compensate for redox reactions occurring at the working electrode.<sup>2,30,31</sup>

Current generated at the working electrode is fed to the inverting input of OA3, which serves as a current follower.<sup>1,31</sup> The output of OA3 is a voltage that is proportional to the current generated at the working electrode (Equation 3), resulting in a signal that is suitable for recording by the data acquisition system.

$$e_o = -i_{work}R3 \quad (3)$$

### *Open-Source Potentiostats*

Various open-source potentiostats have recently been reported (Table 1),<sup>8,27</sup> with costs for components required to build them typically ranging from \$20 to \$200 at the time of publication depending on complexity and quality. In 2019 Guver et al.<sup>29</sup> reported that the cost of materials (excluding the printed circuit board) required to build a DStat<sup>2</sup> was around \$135, a 43% increase compared to the cost reported by Dryden and Wheeler in 2015. While careful inspection of the parts list provided by Guver et al. compared to that which was included with the original DStat report suggests that some of the increase may have resulted from the choice of more costly substitutions, we estimate the material cost associated with the DStat in June 2023 to be \$155 based on the original parts list and \$173 based on the parts list of Guver et al. with a few

integrated circuit parts (i.e., the 16-bit digital-to-analog converter, precision voltage reference, and voltage divider) being most responsible (~60%) for the cost increase over the past four years. The microcontroller required for the DStat has increased by 30% in cost over the same time frame. Though price increases in electronic components in silicon-based integrated circuits have made building open-source instruments more expensive, commercial potentiostats tend to range from hundreds to tens of thousands of dollars depending on capabilities and are also increasing in cost, making open-source instruments appealing alternatives.

The CheapStat, a low cost, hand-held potentiostat developed by Rowe et al. in 2011 was among the first open-source instruments to be reported in the literature. The CheapStat is capable of performing electrochemical experiments like square wave, cyclic, linear sweep, and anodic stripping voltammetries with applications in food and drug quality control, rapid DNA detection and environmental monitoring.<sup>8</sup> The hardware design of the CheapStat includes a three-line Liquid-Crystal Display (LCD) and a joystick by which the user can select a specific technique and set measurement parameters. The instrument can be powered by the USB port of a computer or even a 9 V battery. Data is stored on the device until it can be transmitted to a computer via the USB connection. A Java application was developed by the authors to enable transfer and visualization of the data on a computer. Operation of a potentiostat requires the application of a voltage waveform (i.e., set of continuous analog voltages) between the reference and working electrodes, while the analog current at the WE must be converted to a voltage which can be represented as a digital value, for proper interpretation and analysis. For these operations, the CheapStat makes use of the in-built 12-bit digital-to-analog converter (DAC) (to generate the voltage waveform) and the 12-bit analog-to-digital converter (ADC) (to convert the cell current to a measurable voltage) of the microcontroller.

Table 1. Specifications of Some Selected Open-source Potentiostats and their Material Costs (\$ USD) at the Time of Publication. Theoretical resolutions are based on reported DAC/ADC resolution and voltage/current range. CheapStat, DStat, Meloni, ABE-stat and SweepStat all reported multiple ranges.

Potentiostat	DAC/ADC Resolution (bits)	Voltage Range (Resolution)	Current Range (Resolution)	Cost (\$)
CheapStat <sup>8</sup>	12/12	$\pm 1.0$ V (0.4 mV)	$\pm 10$ $\mu$ A (4.9 nA) $\pm 100$ nA (49 pA)	80
uMED <sup>32</sup>	16/16	$\pm 1.65$ V (50 $\mu$ V)	$\pm 200$ $\mu$ A (5 nA)	25
DStat <sup>2</sup>	16/24	$\pm 1.5$ V (46 $\mu$ V)	$\pm 15$ mA (1.8 nA) $\pm 0.5$ mA (60 pA) $\pm 50$ $\mu$ A (6.0 pA) $\pm 5$ $\mu$ A (0.60 pA) $\pm 0.5$ $\mu$ A (60 fA) $\pm 50$ nA (6.0 fA) $\pm 15$ nA (1.8 fA)	95
Meloni <sup>3,6</sup>	8/10	$\pm 1.0$ V (7.8 mV)	$\pm 200$ $\mu$ A (0.39 $\mu$ A) $\pm 100$ $\mu$ A (0.6 $\mu$ A) $\pm 50$ $\mu$ A (98 $\mu$ A) $\pm 500$ nA (0.98 nA)	30
Dobbelaere et al. <sup>33</sup>	20/22	$\pm 8.0$ V (15 $\mu$ V)	$\pm 2$ $\mu$ A (1.2 pA)	100
UWED <sup>28</sup>	16/10	$\pm 1.5$ V (67 $\mu$ V)	$\pm 180$ $\mu$ A (6.4 nA)	60
JUAMI <sup>34</sup>	8/10	$\pm 2.5$ V (20 mV)	$\pm 10$ mA (10 $\mu$ A)	40
ABE-Stat <sup>35</sup>	16/24	$\pm 1.65$ V (50 $\mu$ V)	$\pm 1.65$ mA (0.20 nA) $\pm 0.165$ mA (19.7 pA) $\pm 16.5$ $\mu$ A (1.97 pA) $\pm 1.65$ $\mu$ A (0.20 pA)	105
SweepStat <sup>36</sup>	12/16	$\pm 1.5$ V (0.73 mV)	$\pm 15$ nA (0.46 pA) $\pm 1.5$ $\mu$ A (46 $\mu$ A)	55
Paqari Stat <sup>27</sup>	8/10	$\pm 1.50$ V (11 mV)	$\pm 225$ $\mu$ A (0.44 $\mu$ A)	23 - 25

The primary operation of a DAC is to convert binary (digital) signals, which are supplied by the microcontroller, to an analog voltage output. While there are different types of DAC configurations, one of the most common is the weighted-resistor ladder DAC (Figure 2).

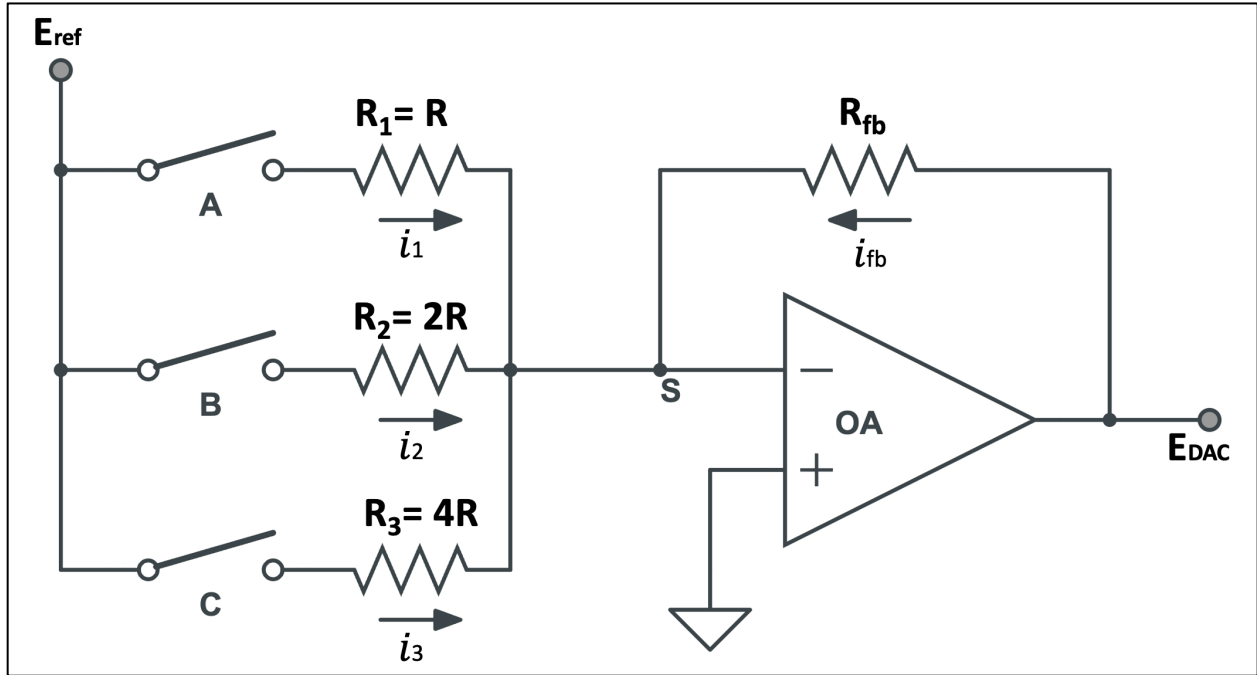


Figure 2. A digital logic circuit of a 3-bit binary-weighted-input DAC.<sup>1</sup>

The resistors in this device are selected to have binary weights (e.g.,  $R$ ,  $2R$ ,  $4R$ , etc.) and are arranged in parallel with one end of each connected to the inverting input of an op amp and the other end of each to an individual switch. All switches are connected on the other side to a common reference voltage ( $E_{ref}$  with respect to ground). The switches are controlled with digital signals, such that the current through any resistor in the ladder ( $R_n$ ) can be either 0 (if the connecting switch is open) or  $\frac{E_{ref}}{R_n}$  (if the connecting switch is closed). The current ( $i_n$ ) through  $R_n$  can be generally expressed by Equation 4.

$$i_n = \frac{E_{ref}}{R_n} X_n \quad (4)$$

where  $X_n$  represents the binary input (0 if open, 1 if closed) used to control the switch connected to  $R_n$ .

A feedback resistor ( $R_{fb}$ , Figure 2) is included in the DAC such that the current at the summing point (S, Figure 2) is given by Equation 5.

$$i_1 + i_2 + i_3 + i_{fb} = \frac{E_{ref}}{R} A + \frac{E_{ref}}{2R} B + \frac{E_{ref}}{4R} C + \frac{E_{DAC}}{R_{fb}} = 0 \quad (5)$$

where A, B, and C represent binary input values associated with switches A, B, and C, respectively.

Rearranging Equation 5 yields an expression for  $E_{DAC}$  in terms of  $E_{ref}$ , binary inputs and resistor values (Equation 6).

$$E_{DAC} = -E_{ref} R_{fb} \left( \frac{A}{R} + \frac{B}{2R} + \frac{C}{4R} \right) \quad (6)$$

From equation 6, it can be seen that the logic value of the switch connected to the lowest resistance (A) represents the most significant bit (MSB) since it has the largest effect on the output, while the logic value of the switch connected to the highest resistance (C) is the least significant bit (LSB). Generating an analog output from  $E_{ref}$  using a DAC involves providing the appropriate logic values to the switches (Table 2). The resolution of the DAC is 1 part in  $2^n$  and defines the possible steps in voltage that can be generated at the output. Therefore, a DAC with a large number of inputs would have a high resolution (many steps) and lead to a smoother analog signal at the output. The analog voltage generated by the DAC is provided as an input for the potentiostatic control unit of a potentiostat (Figure 1).

Table 2. Example of Output from a 3-bit Weighted-resistor Ladder DAC. In this case,  $R_1 = 7R$ ,  $R_2 = 14R$ ,  $R_3 = 28R$ , and  $R_{fb} = 4R$  such that the output range is from 0 to  $-E_{ref}$ . A, B and C represent binary values for switches.

A	B	C	Binary Number	$E_{DAC}, V$
0	0	0	000	0
0	0	1	001	$-\frac{E_{ref}}{7}$
0	1	0	010	$-\frac{2E_{ref}}{7}$
0	1	1	011	$-\frac{3E_{ref}}{7}$
1	0	0	100	$-\frac{4E_{ref}}{7}$
1	0	1	101	$-\frac{5E_{ref}}{7}$
1	1	0	110	$-\frac{6E_{ref}}{7}$
1	1	1	111	$-E_{ref}$

In 2015, Dryden and Wheeler reported a general-purpose open-source lab potentiostat (DStat) that is capable of high precision, low noise measurements, with performance comparable to many high-quality commercial instruments. Though the microcontroller used in the DStat features a 12-bit built-in DAC like that upon which the potentiostatic control circuit of the CheapStat is based, the DStat circuit design instead interfaces an external 16-bit DAC with the microcontroller for superior potentiostatic control. In addition to employing a DAC of higher resolution, the DAC voltage is also passed through an active 4<sup>th</sup> order low-pass reconstruction

filter. These features result in the ability of the DStat to produce a high resolution ( $46 \mu\text{V}/\text{step}$ ) voltage waveform with great accuracy at high frequencies and reduced noise within the operating limits of  $+1.5$  to  $-1.5 \text{ V}$ .<sup>2</sup> A high resolution 24-bit ADC is also interfaced with the microcontroller in the DStat design, thereby, enabling measurements of current with great precision. An 8:1 multiplexer included in the DStat's current-to-voltage convertor provides eight possible current ranges, which are defined by the values of feedback resistor options ( $0 \Omega$ ,  $100 \Omega$ ,  $3 \text{ k}\Omega$ ,  $30 \text{ k}\Omega$ ,  $300 \text{ k}\Omega$ ,  $3 \text{ M}\Omega$ ,  $30 \text{ M}\Omega$ , and  $100 \text{ M}\Omega$ ) included in the current follower part of the circuit.<sup>2</sup>

To enable accurate measurement of low electrochemical cell currents, op amps with very low input bias currents were selected in the hardware design of DStat. The input bias current for the dual op amp used in the potentiostatic control circuit is  $\sim 200 \text{ fA}$ , while that for the internally-compensated single op amp (shielded to achieve low current measurements) used in current-to-voltage convertor is  $3 \text{ fA}$ . In addition, both the potentiostatic control circuit and current-voltage-converter are referenced to a high precision voltage reference instead of a voltage generated using a regulator powered by the on-board power supply since fluctuations in on-board power can be a significant source of noise.<sup>2</sup>

To fabricate a simple, cheap, and easily customizable open-source potentiostat suitable for undergraduate education, Meloni developed an inexpensive instrument based on the popular Arduino Uno microcontroller development board.<sup>3</sup> While the microcontroller chips employed in other open-source potentiostats like CheapStat and DStat must be programmed with firmware supplied by the creator or adapted by the builder, use of a pre-programmed microcontroller development board like those offered by Arduino presents a quicker, easier route to developing instruments.

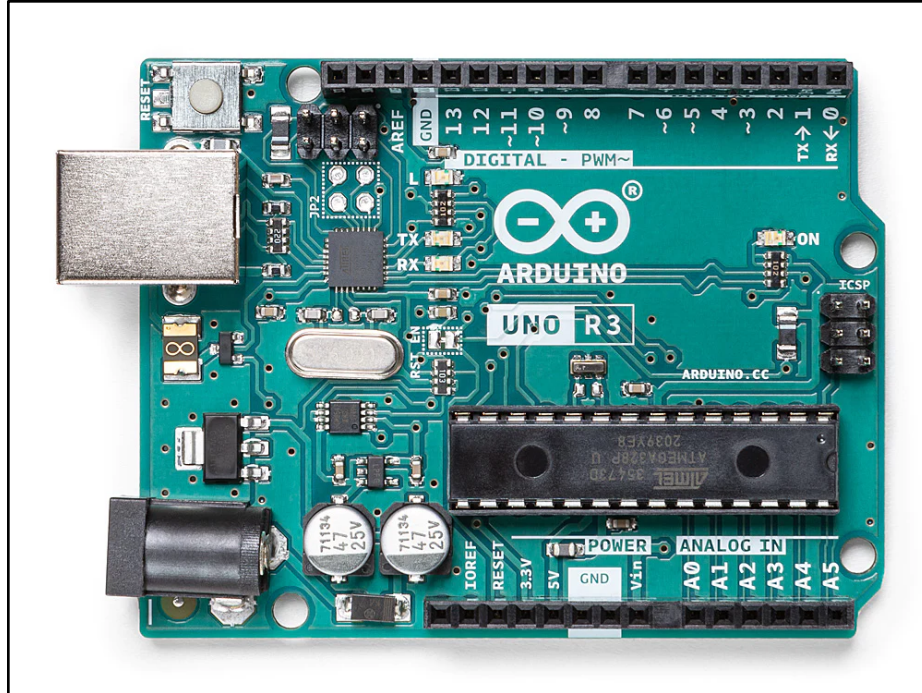


Figure 3. An image of an Arduino Uno development board. Reproduced from the Arduino Creative Commons Platform.<sup>37</sup>

Arduino development boards contain headers to easily connect peripheral circuitry of the instrument to the microcontroller and can also be interfaced with free, easy-to-use integrated development environment (IDE) software. One can write scripts or sketches (in a C++ programming language) in the IDE to define the instructions for the microcontroller, which can then be uploaded to the development board via the USB interface.

Since the Arduino Uno does not contain a built-in DAC, analog voltages required for potentiostatic experiments in Meloni's design are generated using pulse-width modulation (PWM). In PWM, a square wave that alternates between the digital high and low voltages is controlled to provide an output that ranges between these two digital signals and corresponds to the average voltage over the full cycle time (Figure 4). The output voltage is simply the product

of high state voltage and the duty cycle, which is the fraction of time the square wave spends in the high state compared to the time of one full cycle.

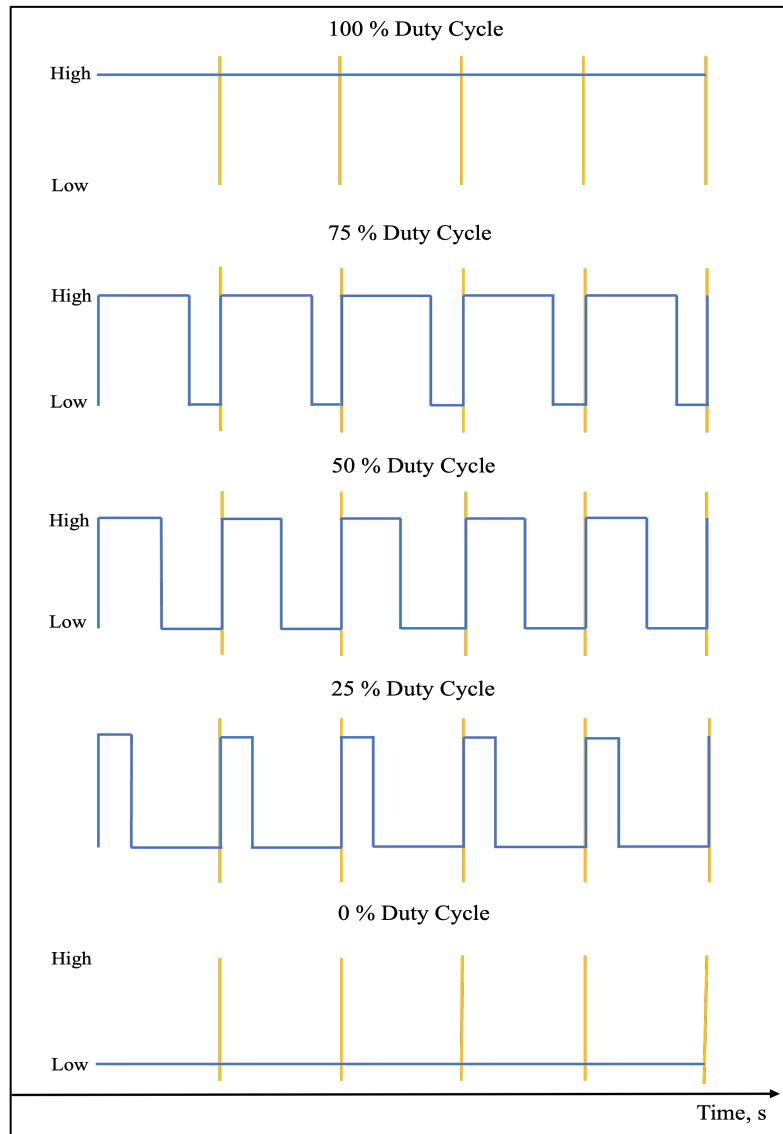


Figure 4. Illustration of Pulse Width Modulation (PWM). Duty cycles of 0 to 100 % are shown to illustrate the amount of time the signal stays high (on) relative to the full cycle time.

The resolution of the PWM channels on the Arduino Uno used by Meloni is 8-bit, permitting the output to provide 256 different voltages ranging between 0 and 5 V (operating voltage of the Uno). By combining the PWM output with a bias voltage of -5 V and using

resistors to shift the voltage level in the potentiostatic control circuit, Meloni's Uno-based potentiostat is capable of operating at voltages between  $\pm 1$  V with a resolution of 7.8 mV/step.

While the op amps utilized in the CheapStat and DStat are supplied with power derived from the USB port of a computer, powering the quad op amps in Meloni's Uno-based design requires the use of a separate symmetric  $\pm 12$  V dual supply. As Meloni reported, an ATX power supply salvaged from an old personal computer can be used to provide this function in place of a more expensive lab power supply to reduce costs.<sup>3</sup> The Arduino Uno microcontroller development board is powered separately by a computer via the USB port interface.

While Meloni's design does not incorporate a multiplexer in the current-to-voltage convertor like the one featured in Dryden and Wheeler's DStat, flexibility in the useable current range is accomplished by selection of the bias and feedback resistors in the current follower part of the circuit. Meloni reported useable ranges of  $\pm 200$   $\mu$ A to  $\pm 500$  nA for the Uno-based instrument, which was originally built on a simple breadboard but converted into a simple printed-circuit board (PCB) format designed for through-hole components. The PCB format features headers to connect a smaller circuit board module (called a "shield"), which contains the bias and feedback resistors for adjusting the current range. Interestingly, Meloni also introduced a separate set of resistors on the shields to form a voltage divider so the Uno could recognize which resistor combination was attached to the current-to-voltage convertor and set the correct current range for ADC.

### *Research Aims*

Interest in open-source potentiostats has continued to increase since the initial release of the CheapStat in 2011. These instruments offer low-cost alternatives to more expensive commercial options, high value in developing and demonstrating electronics and coding skills as

well as principles of instrument design in teaching environments, and the possibility to interface with other accessories or equipment for novel techniques or applications. Here, we develop and demonstrate simple, low-cost potentiostats based on the Arduino Nano Every microcontroller development board. The potentiostats are constructed on breadboards and designed such that no additional external power supply is needed for the integrated circuits. The two different designs feature different potentiostatic control circuits, one that utilizes pulse-width modulation (PWM) and another that employs an external digital-to-analog converter (DAC). Performance of the home-built potentiostats are compared to one another and to a commercial instrument by evaluating the relationship between applied voltage and current measured across selected resistances. The electrochemical responses of the instruments are also compared through experiments that employ glassy carbon and home-built pencil graphite working electrodes.

## CHAPTER 2. EXPERIMENTAL

### *Materials*

Nano Every microcontroller boards were obtained from Arduino. Most of the required electronic components (integrated circuits, resistors, capacitors, etc.) were obtained from Digi-Key or Mouser. The MCP4725 DAC breakout board from Commidox was purchased from Amazon. Potassium ferricyanide and ferrocene methanol redox probes were obtained from Fisher Scientific. Potassium chloride and sodium chloride were obtained from Acros Organic. B9R-4-Yellow photopolymer resin was procured from B9Creations. All solutions were prepared using 18.2 M $\Omega$  cm ultrapure water that was obtained by passing deionized water through Millipore Synergy UV water purification system.

### *Pencil Graphite Electrode Fabrication*

Electrodes were fabricated by integrating pencil graphite rods (0.5 mm diameter) and metal wires with the help of a conductive silver paste into commercially available fitting.<sup>39,40</sup> As previously reported,<sup>41</sup> each fitting consisted of three working pencil graphite electrodes, a reference electrode made from 0.25 mm silver wire coated with silver chloride and a counter electrode built from a 16 G stainless steel needle. Teflon tape was used to insulate the exposed copper wire to avoid short-circuiting adjacent electrodes. Ring-shaped counter electrodes were built from the barrel of a 16G stainless-steel needle. Reference electrodes were prepared by winding silver wire around an exposed copper wire. Conductive silver paste was again used to facilitate connection, and Teflon tape was wrapped around the copper-silver wire junction to avoid shorts when placed in the void-space of the ring-shaped stainless-steel counter electrode. The resistances of the electrodes were inspected with multimeter and found to be in the range of 0 – 9  $\Omega$ .

Prior to insertion in commercial fitting, electrodes, were placed in a 3D printed electrode spacer which was developed in-house to accommodate each electrode and to prevent short-circuits. The spacer is a cylinder that fits inside a commercial fitting and contains equally distributed holes designed for placing electrodes. Gaps in between the electrodes and spacer walls, and the spacer and fitting were sealed with epoxy. The assembled electrodes were polished on a 600-grit abrasive paper after curing to expose the disk-shaped electrodes for electrochemical analysis.

After sealing with epoxy and polishing, resistances of each electrode were inspected again to ensure complete connection and check for shorts. This was done by hooking one end of the probe on a multimeter to the exposed electrode and making a contact with the other probe on the exposed copper wire on the other side.

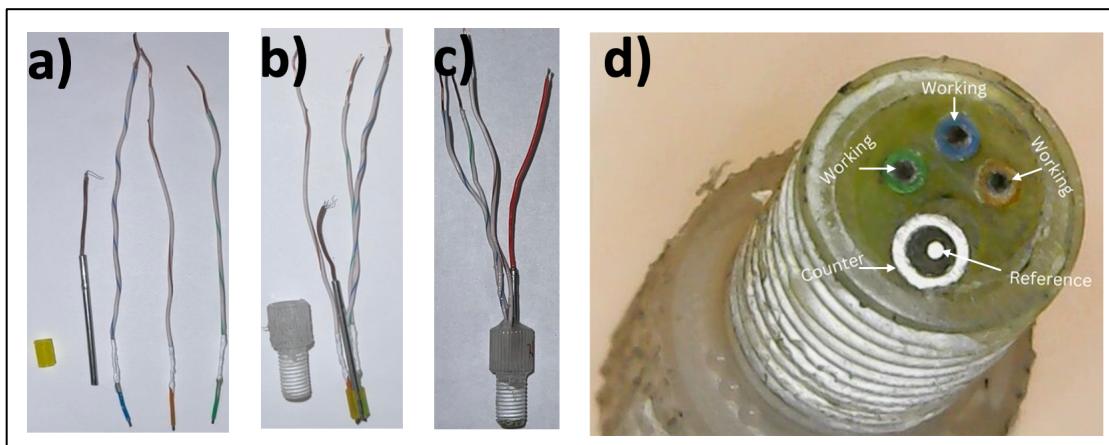


Figure 5. Assemble of pencil graphite electrode (PGE) arrays. A) Materials used to prepare PGE arrays. (From left-to-right) 3D-printed electrode spacer (yellow), stainless steel open cylinder counter electrode with silver wire reference electrode inside, and three working PGEs attached to copper wire leads. B) Electrodes in 3D-printed spacer next to commercial fitting. C) Electrodes assembled in commercial fitting. D) View of electrodes in fitting.

Prior to electrochemical measurement and characterization of fabricated electrodes, the silver metal disk-shaped reference electrode was coated with silver chloride to provide a suitable quasi-reference electrode for the system. To achieve this, the electrode was immersed in a 3.5 M KCl solution, and the silver metal reference lead was connected to a 1.0 M $\Omega$  resistor that was attached on the other end to the cathodic part of a 9 V battery.<sup>41</sup> To complete the circuit, a commercially available silver chloride-coated silver wire was immersed in the same solution and connected to the anodic part of the 9 V battery. The set-up was allowed to sit for about thirty-five minutes until the shiny silver wire in the fitting turned gray.<sup>41</sup> Open-circuit potential of the coated silver wire was measured in 1 M KCl against a commercial CH instrument Ag/AgCl reference electrode that was filled with 1 M KCl solution.

#### *Electrochemical Characterization*

Resistor tests and electrochemical experiments were conducted using home-built potentiostats and a commercial CH Instruments 760E electrochemical workstation for comparison. For resistor tests, the reference and counter leads of the instrument were short-circuited by connecting both to one side of the resistor, while the working electrode lead was connected to the other side of the resistor. A linear voltage sweep from 2.5 to -2.5 V was applied between the reference and working electrodes.

All cyclic voltammetry (CV) experiments were conducted in 10 mM potassium ferricyanide ( $\text{K}_3\text{FeCN}_6$ ) with 0.1 M KCl supporting electrolyte using a 3 mm glassy carbon working electrode (CH Instruments) with platinum wire counter and silver-silver chloride reference (CH Instruments, 1 M KCl filling solution). In separate CV experiments, measurements in 10 mM  $\text{K}_3\text{FeCN}_6$  with 0.1 M KCl were repeated using the home-built pencil graphite electrode assemblies (PGE) with one of the PGEs serving as the working electrode,

AgCl-coated Ag as the reference and stainless steel as the counter. All CV data were processed in CH Instruments software to determine peak currents.

## CHAPTER 3. RESULTS AND DISCUSSION

### *Hardware Development of Home-built Potentiostats*

Potentiostat designs were inspired by previously reported open-source instruments with some modifications.<sup>2,3,27,35</sup> The home-built potentiostats were based on an Arduino Nano Every development board, which utilizes an ATmega4809 microcontroller. Much like the Arduino Uno that is utilized in the potentiostat previously developed by Meloni,<sup>3</sup> the Nano Every operates at 5 V and features a built-in 10-bit ADC but has a smaller footprint (45 mm x 18 mm for the Nano Every vs. 68.6 mm x 53.3 mm for the Uno). Since the Nano Every (like the Uno) does not have a built-in DAC, the output voltage is provided through use of one of the microcontroller's 8-bit PWM outputs or, alternatively, an external 12-bit DAC (MCP4725) controlled by the Nano Every.

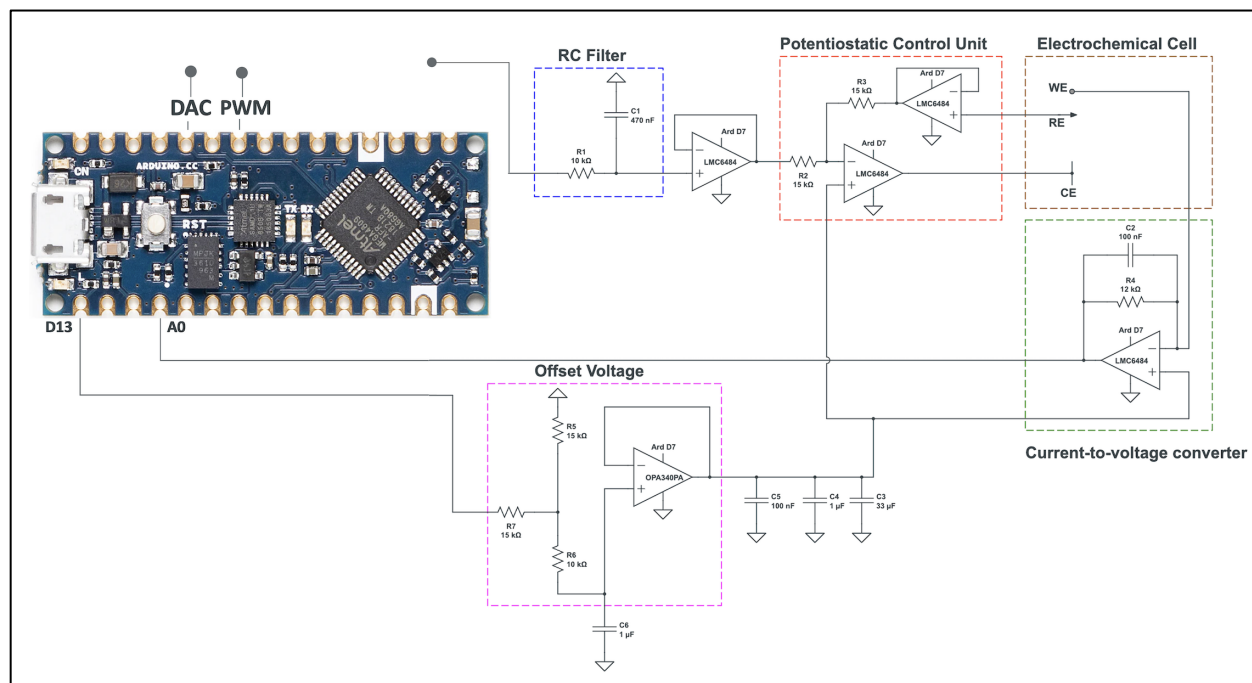


Figure 6. Simplified circuit diagram of compact, home-built PWM- and external DAC-based electrochemical analyzers.

For both Nano Every potentiostat designs, the voltage supplied by either PWM or the external DAC is filtered using a simple, passive low-pass RC filter<sup>3,27</sup> as is consistent with previously reported Arduino-based potentiostats developed by Meloni (Arduino Uno)<sup>3</sup> and Cordova et al. (Arduino Nano)<sup>27</sup>. The low-pass RC filter attenuates and effectively removes high frequency components of the signal, which are more susceptible to noise. The ability of the RC filter to attenuate high frequency components is characterized by its cut-off frequency ( $f_c$ ), which is defined as the frequency at which the output voltage is -3 dB of the input voltage (i.e.,  $e_{out} = 0.707 * V_{in}$ ).  $f_c$  is related to values of R and C, for which the product RC represents the RC time constant, by Equation 7.<sup>3</sup>

$$f_c = \frac{1}{2\pi RC} \quad (7)$$

A lower  $f_c$  (higher RC time constant) results in a smoother (i.e., reduced noise) output since more high frequency components are removed. However, lowering  $f_c$  also increases the rise time ( $t_r$ ) (Equation 8) of the circuit, which is defined as the span of time it takes for the filter to respond to an abrupt change in input voltage by increasing its output to values beginning at 10% and ending at 90% of the new input.

$$t_r = \frac{0.35}{f_c} \quad (8)$$

Due to the dependence of  $t_r$  on  $f_c$ , an instrument with a low cutoff frequency responds more slowly to changes in input signal, while a higher cut-off frequency enables faster experiments. The RC filter for the Nano Every potentiostats consists of a 10 k $\Omega$  resistor and a 470 nF capacitor connected in series (adapted from Meloni) which provides an  $f_c$  of 33.86 Hz and a  $t_r$  of 10.3 ms.  $t_r$  represents the lower limit at which the PWM or DAC value can be changed. Thus, it determines the upper limit of the voltage scan rate.<sup>3</sup>

While the designs of both Meloni and Cordova et al.<sup>3,27</sup> utilized low-cost LM324 quad op amps, we employ an LMC6484 quad op amp in the Nano Every potentiostats, which features a lower input bias current (0.02 pA vs. 90 nA), making it more suitable for experiments that involve low-current measurements. Additionally, unlike previously reported designs which power the LM324 using a symmetric dual power supply, the LMC6484 can be powered from a single supply with a potential as low as 3V, like that provided by a common coin cell battery.<sup>36</sup>

The LMC6484 quad op amp employed in the Nano Every potentiostats is the same as that which was previously employed by Glasscott et al. in their two-electrode potentiostat called SweepStat. The SweepStat is based on a Teensy 3.2 microcontroller development board<sup>36</sup> and was designed for chemical education with the two-electrode configuration adopted for simplicity, to reduce cost, and to demonstrate the effects of iR potential drop (for which the reference electrode is included in 3-electrode instruments to compensate) on voltammetric responses. However, it is worth mentioning that instrument control and experimental data collection for the SweepStat is accomplished through an interface based on costly third-party software (National Instruments LabView).<sup>36</sup>

Potentiostatic control in the Nano Every-based electrochemical analyzers (Figure 5) is based on the classic adder potentiostat design (Figure 1).<sup>31, 2,31,35</sup> However, this part of the circuit had to be adapted to adjust the usable range of the instrument into one which is consistent with common electrochemical experiments.<sup>2,35</sup> Since the Nano Every's operating potential is 5 V, the built-in ADC is configured for inputs of 0 to 5 V and the PWM output is also 0 to 5 V, which defines the usable range of the microcontroller. While the upper limit of the external DAC output can be adjusted by providing a voltage between 2.7 and 5.5 V to the DAC input, the DAC was supplied with 5 V from the Nano Every such that the output also ranges from 0 to 5 V for

consistency with PWM operation. Since electrochemical experiments can require both positive and negative potentials to be applied between the working and reference electrodes, PWM and DAC outputs, which range from 0 to 5 V, must be level-shifted<sup>36</sup> to provide this capability. By applying an offset voltage ( $E_{offset}$ ) to the non-inverting input of the potentiostatic control unit (Figure 5), the potential of the reference electrode ( $E_{RE}$ ) can be controlled with respect to ground by adjusting the PWM or DAC voltage ( $E_{PWM/DAC}$ ) (Equation 9).<sup>31</sup>

$$E_{RE} = E_{offset} - E_{PWM/DAC} \quad (9)$$

$E_{offset}$ , which is generated using a microcontroller-supplied voltage fed through to a voltage divider,<sup>2</sup> was chosen to be  $\frac{1}{2} * E_{PWM/DAC}$  (in this case, 2.5 V) to enable a symmetric potential window. Since  $V_{DAC}$  can only range between 0 V and 5 V, a potential window of  $\pm 2.5$  V (5 V full-scale voltage range) is achieved. This results in potential step ( $E_{step}$ ) resolutions for PWM- and external DAC-based builds of 19.6 mV/step and 1.2 mV/step, respectively (Equation 10)<sup>30</sup>

$$E_{step} = \frac{E_{FSR}}{2^n - 1} \quad (10)$$

where  $n$  is the number of bits of the DAC/PWM and  $E_{FSR}$  is the full-scale voltage range.

Current that passes through the working electrode as a result of electrochemical reactions (i.e., Faradaic current) or non-Faradaic processes is fed into a current follower op amp through the inverting input where current is converted to voltage (Equation 3) so that it can be interpreted by the Nano Every's built-in 10-bit.<sup>2,35</sup> Since the ADC can only read voltages from 0 V to 5 V and  $E_{work} = i_{work} R_4$  ranges between +2.5 V and -2.5 V (vs.  $E_{RE}$ ) due to the potentiostatic control circuit design, a 2.5 V offset voltage is supplied to the noninverting input of the current follower (Equation 11).<sup>3</sup>

$$E_{ADC} = E_{offset} - i_{work} R_4 \quad (11)$$

Since  $E_{offset} = \frac{1}{2}E_{ADC,max}$ , the current range of the current-to-voltage convertor is symmetric, ranging from  $-\frac{1}{2}E_{ADC,max}/R_4$  to  $\frac{1}{2}E_{ADC,max}/R_4$ .  $R_4$  (the value of the feedback gain resistor) in the home-built Nano Every potentiostats was chosen to be 12 or 50 k $\Omega$  corresponding to a useable current ranges of  $\pm 208 \mu A$  or  $\pm 50 \mu A$ , respectively. The usable current range can be adjusted by changing the value of  $R_4$ . Both PWM and external DAC versions of the home-built Nano Every potentiostats were constructed on breadboards (Figure 7).

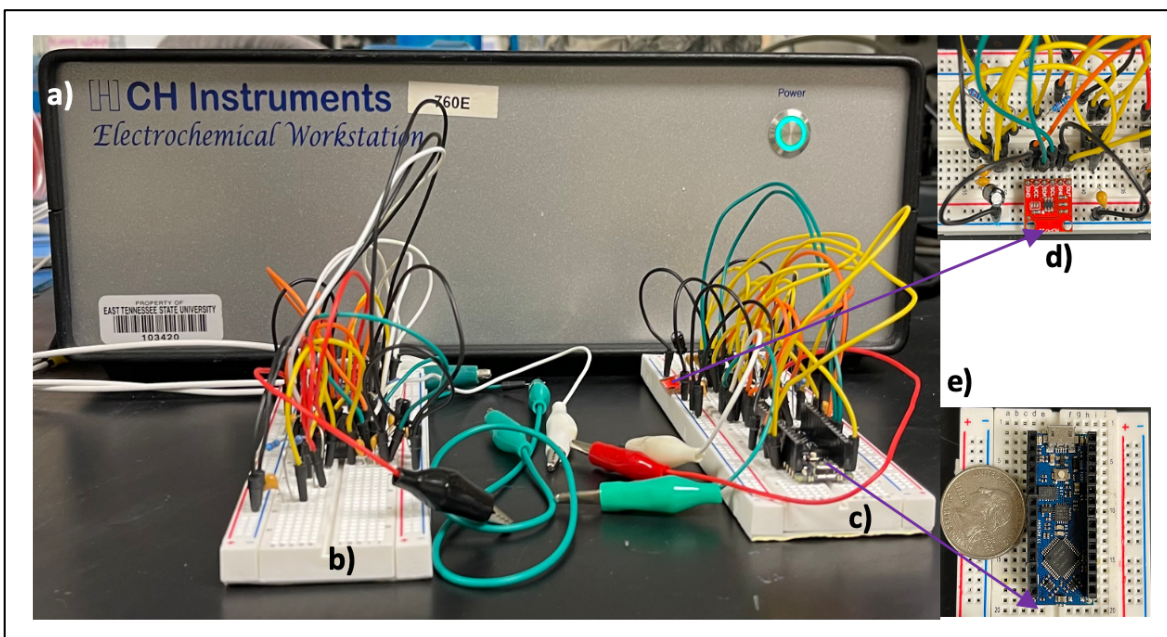


Figure 7. Photographs of commercial (CH instruments 760E Electrochemical Workstation) and home-built electrochemical analyzers based on an open-source microcontroller. A) Commercial instrument. B) Breadboard-based electrochemical analyzer that utilizes pulse-width modulation (PWM). C) Breadboard-based electrochemical analyzer that uses an external digital-to-analog (DAC) converter. (d) MCP4725 external DAC. Both breadboard-based electrochemical analyzers utilize the open-source Arduino Nano Every microcontroller.

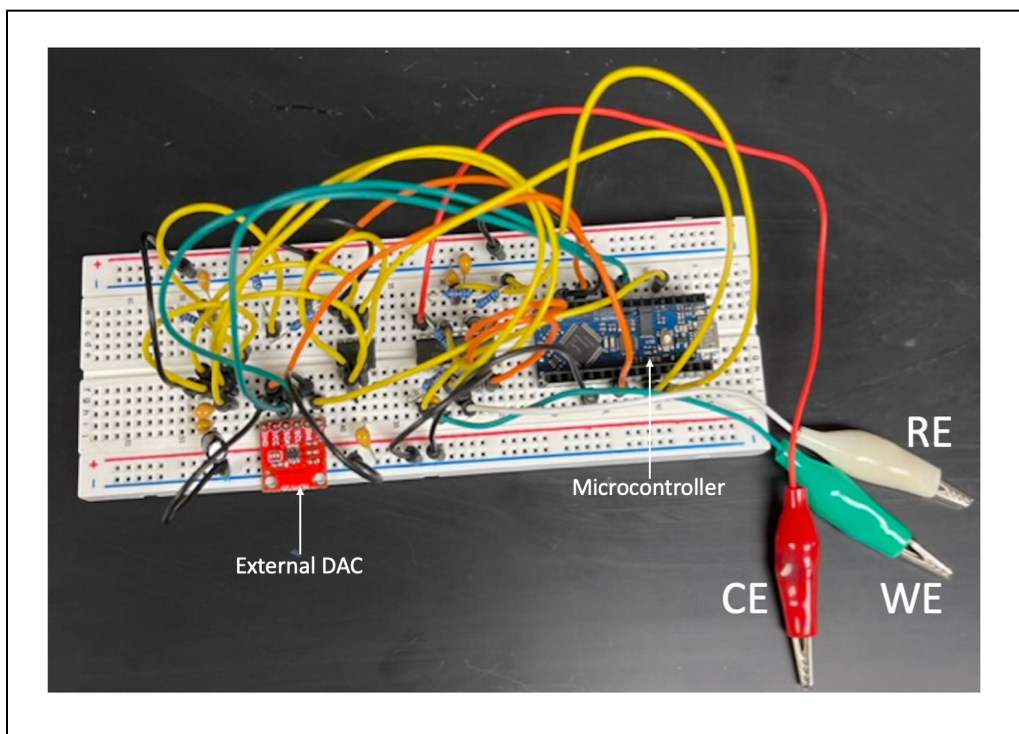


Figure 8. Top-view of components assembled on a breadboard for external DAC-based instrument.

### *Software Development*

Home-built open-source electrochemical analyzers were interfaced with the Arduino IDE software via the USB port. Sketches/codes were written in Arduino programming language (based on C++) in the IDE to facilitate voltammetric sweep experiments. In a voltammetric sweep experiment like linear sweep or cyclic voltammetry, the potential of the working electrode (with respect to the reference) is changed at a user-defined rate from a user-defined starting value to a user-defined ending or switching value (Figure 9a), while current associated with processes at the working electrode is continuously sampled. This process may be repeated in the opposite direction to complete a cyclic sweep. Achieving the potential output for such experiments via PWM or a DAC requires setting the PWM/DAC value to one that corresponds to the desired starting potential (Figure 9b) holding that value for a time that is determined by the sweep or

scan rate and the resolution of the PWM/DAC, sampling the current, incrementing or decrementing the PWM/DAC value in the direction of the desired end or switching potential, and repeating hold, sampling, and PWM/DAC adjustment steps until the scan of the user-defined voltage range is complete.

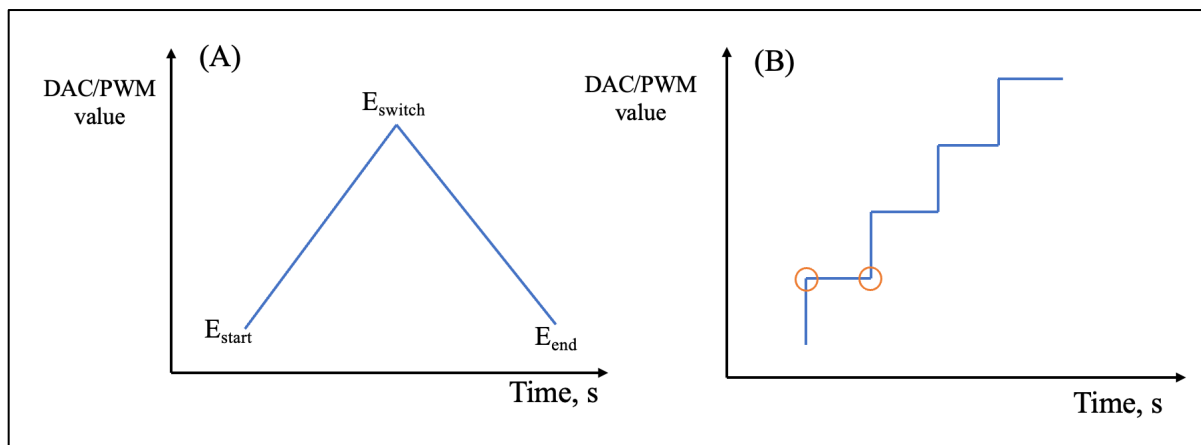


Figure 9. Illustration of DAC/PWM value – time plot. A) Change in DAC/PWM value from  $E_{start}$  to  $E_{end}$ . B) A detailed view of Part A where circled regions show time delay for current measurement.

The code for voltammetric sweep experiments with the Nano Every potentiostats (Appendices A and B) was developed based on Meloni's Uno code<sup>3</sup> with some modifications. The sketch allows the user to define parameters for scan rate (in mV/s), starting potential ( $E_{start}$  in mV), switching potential ( $E_{switch}$  in mV), and ending potential ( $E_{end}$  in mV) for the desired experiment (Figure 8). User-defined potentials ( $E_D$ ), which include  $E_{start}$ ,  $E_{switch}$ , and  $E_{end}$ , are converted to equivalent DAC/PWM values ( $E_{DAC/PWM}$ ) based on the potential step resolution (Equation 10) according to Equation 12.

$$E_{DAC/PWM} = (2^n - 1) + \frac{(E_D - E_{offset})}{Potential\ Step} \quad (12)$$

where  $n$  is the number of bits of the DAC/PWM and  $E_{\text{offset}}$  is the offset voltage supplied to the potentiostatic control circuit (in this case, 2500 mV).

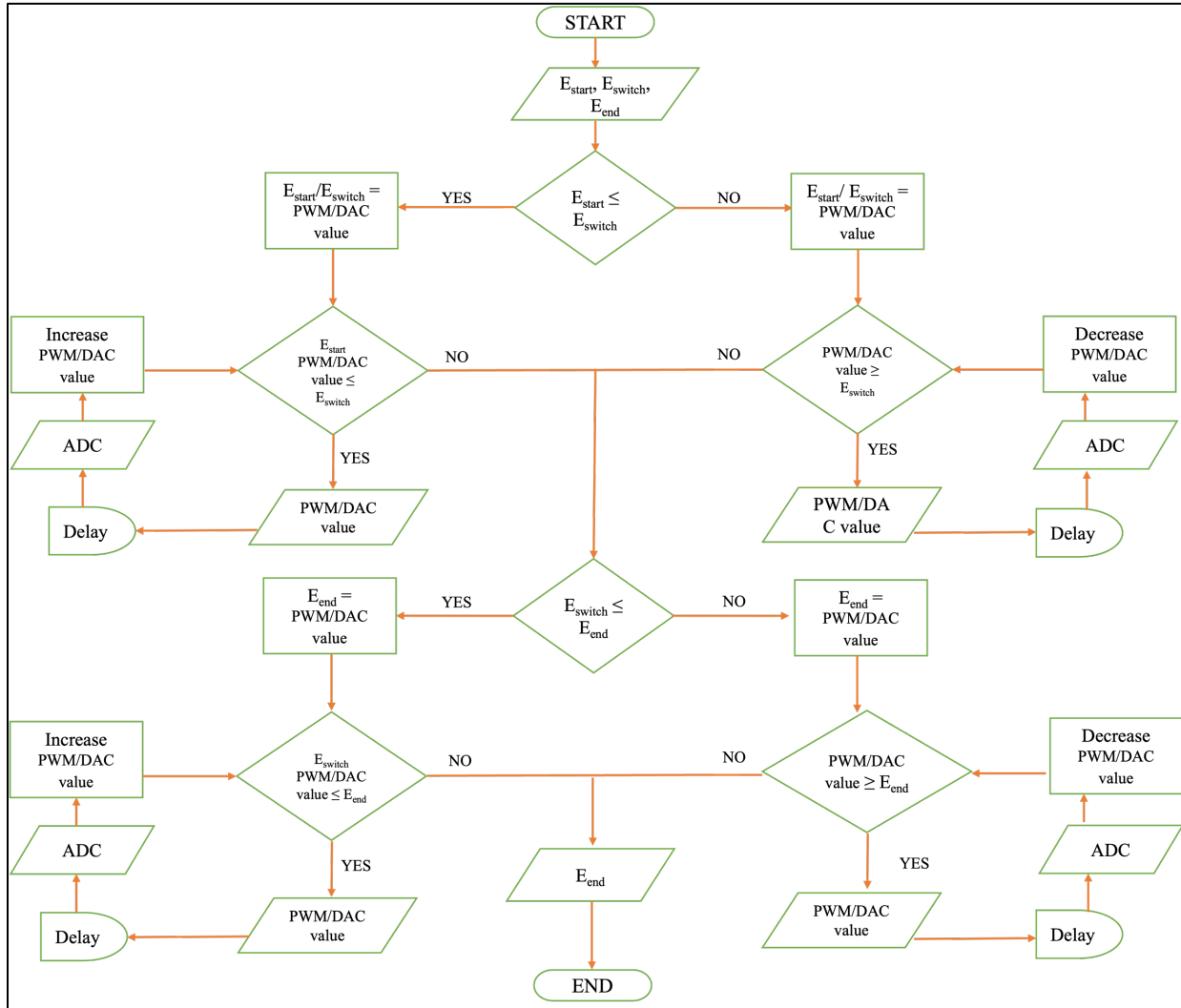


Figure 10. A flowchart representation of sketch uploaded onto microcontroller.

The program proceeds into a loop where, 1)  $E_{\text{start}}$  is converted to its corresponding DAC/PWM value; 2) the microcontroller or external DAC outputs the appropriate value for a length of time that is determined by the user-defined scan rate and the step resolution (Equation 13); 3) the value of the microcontroller's built-in ADC input (output of the potentiostat's current-to-voltage convertor) is recorded and converted to current (Equation 11); 4) the DAC/PWM

value is either incremented or decremented (depending on whether  $E_{\text{switch}}$  is greater than or less than  $E_{\text{start}}$ ) towards the switching potential; and steps 2-4 are repeated until the current at  $E_{\text{switch}}$  has been measured. For cyclic voltammetry experiments, after measurement of the current at  $E_{\text{switch}}$ , step 1-4 will be repeated with  $E_{\text{switch}}$  and  $E_{\text{end}}$  in the places of  $E_{\text{start}}$  and  $E_{\text{switch}}$ , respectively.

$$t_{\text{step}} = \frac{1000E_{\text{step}}}{\text{rate}} \quad (13)$$

where  $E_{\text{step}}$  is in mV/step (or V/step) and rate is in mV/s (or V/s) and the result  $t_{\text{step}}$  is a delay in ms.

### *Current-Voltage Measurements with Commercial and Home-built Instruments*

#### *Resistor Tests*

To evaluate current-voltage (I-V) relationships of the Nano Every potentiostats, resistors were connected between the working and reference/counter (physically shorted) electrode leads and linear sweep voltammetry at a sweep rate of 50 mV/s. Results for such experiments are expected to follow Ohm's law ( $V = IR$ ),<sup>1</sup> yielding a linear I-V relationship with a slope consistent with  $1/R$ . Experiments were performed with 12 k $\Omega$ , 50 k $\Omega$  and 100 k $\Omega$  resistors (tolerances  $\pm 1\%$ ) (Figure 11), which were evaluated using linear sweep voltammetry with a commercial CH Instruments 760E electrochemical analyzer to obtain accurate resistance values to which results from home-built potentiostats are compared.

As expected, all three instruments gave linear relationships between current and applied voltage (Figure 11a). The commercial instrument features a 16-bit DAC, which enables more closely spaced potential steps than those of the home-built potentiostats (Figure 11b). A potential step resolution of 1 mV (the default value) was employed in measurements with the commercial instrument, while the potential step resolutions for the PWM and external DAC versions of the

home-built instruments were 19.6 and 1.22 mV (Equation 10), respectively, as limited by the circuit designs.

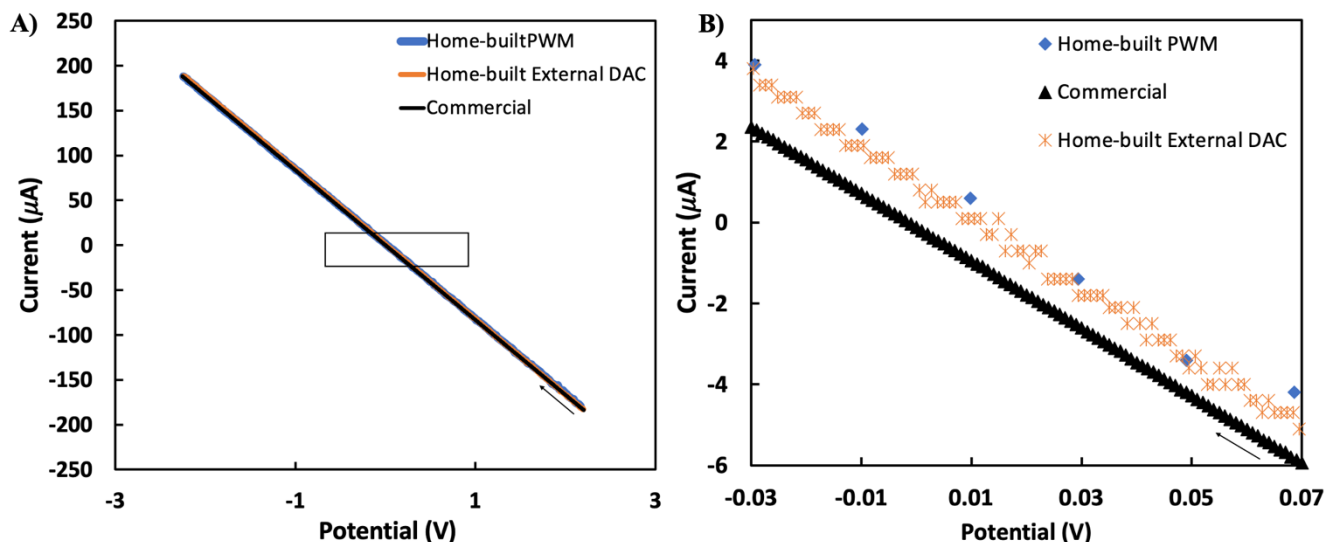


Figure 11. Linear sweep voltammogram of a 12 k $\Omega$  resistor at 50 mV/s. A) Comparison of results from all three instruments. B) Detailed view of boxed region of plot in (a). Arrow indicates direction of scan.

Closer inspection of the I-V data (Figure 11b) also reveals a small offset in the current responses of the home-built potentiostats compared to that of the commercial instrument. These discrepancies may be attributed to the more limited voltage and current resolutions of the home-built instruments. Aside from DAC/PWM-related differences in potential application, the home-built potentiostats employ the Nano Every's built-in 10-bit ADC, which results in a theoretical limit in current resolution of 0.098% (i.e.,  $2^{10}$ ) of the full current range (e.g., 0.39  $\mu$ A for the  $\pm 208$   $\mu$ A range provided using a 12 k $\Omega$  feedback resistor in the current-to-voltage convertor, Equation 11).<sup>3</sup> For comparison, the commercial instrument utilizes a 16-bit ADC, which is capable of measuring currents at the theoretical limit of 0.0015% of the full current range.

Table 3. Comparison of Resistor Test Results for Home-built Instruments at 50 mV/s. Resistors with 1% tolerance were used for all tests. Test resistance values (R) were determined from the linear slopes of current-voltage curves obtained using a commercial CH Instrument 760E.

<b>R (kΩ)</b>	<b>Potentiostat</b>	<b>I-V slope (± uncertainty) (μA/V)</b>	<b>Calculated Resistance (± uncertainty) (kΩ)</b>	<b>% Error</b>
12.00000	PWM	-83.10 (± 3.0 x 10 <sup>-2</sup> )	12.000 (± 5.0 x 10 <sup>-3</sup> )	0
	External DAC	-83.800 (± 8.0 x 10 <sup>-3</sup> )	11.900 (± 1.1 x 10 <sup>-3</sup> )	-0.83
49.8000	PWM	-19.70 (± 4.3 x 10 <sup>-2</sup> )	50.7 (± 1.1 x 10 <sup>-1</sup> )	1.80
	External DAC	-20.000 (± 6.6 x 10 <sup>-3</sup> )	49.90 (± 1.7 x 10 <sup>-2</sup> )	-0.20
100.0000	PWM	-9.80 (± 2.6 x 10 <sup>-2</sup> )	102.6 (± 2.7 x 10 <sup>-1</sup> )	2.6
	External DAC	-9.900 (± 5.0 x 10 <sup>-3</sup> )	100.50 (± 5.0 x 10 <sup>-2</sup> )	0.50

Due to the high precision of the commercial instrument, slopes of I-V measurements of resistors obtained with the commercial instrument were used to determine the corresponding resistance according to Ohm's law. Performances of home-built instruments were evaluated by similarly determining resistance from I-V measurements and comparing to that which is obtained from the commercial instruments (Table 3). Resistance values determined using the home-built instruments were within 3% for all resistors. The external DAC version exhibited less variation in performance with all resistors measuring within -0.83% to +0.50% of their accepted values compared to the PWM version (0% to 2.6%).

*Electrochemical Characterization of Commercial and Home-built Instruments*

Cyclic voltammetry (CV) experiments were carried out in 10 mM potassium ferricyanide ( $\text{K}_3\text{FeCN}_6$ ), a common redox probe,<sup>42</sup> with 0.1 M KCl supporting electrolyte within a potential range of 0.7 to -0.4 V at varying scan rates from 10 to 100 mV/s to compare electrochemical responses of home-built potentiostats to those from a commercial instrument (CH Instruments 760E). With a commercial 3 mm glassy carbon (GC) working electrode, platinum wire counter and Ag/AgCl reference, both home-built potentiostats exhibited the expected peak-shaped response for the one-electron  $[\text{FeCN}_6]^{3-/4-}$  redox couple,<sup>43</sup> similar to that obtained with the commercial (Figure 12A).

The Randles-Sevcik equation (Equation 14), which relates the peak current ( $i_p$ ) to scan rate ( $v$ ), number of electrons involved in the redox reaction ( $n$ ), area of the electrode ( $A$ ), concentration of the redox-active species in the bulk solution ( $C$ ), and diffusion coefficient of the redox species ( $D$ ) was used to determine  $D$  for  $[\text{FeCN}_6]^{3-}$  from CV data obtained using the commercial and home-built potentiostats.

$$i_p = (2.69 \times 10^5) n^{3/2} A D^{1/2} C v^{1/2} \quad (14)$$

Peak currents of CVs for all experiments were determined using CHI software.  $A$  of the GC electrode was determined to be 0.065 cm<sup>2</sup> based on ImageJ analysis of a photograph of the disk-shaped electrode. Based on the slopes of the Randles-Sevcik plots (Figure 12b),  $D$  for  $[\text{FeCN}_6]^{3-}$  was found to be  $7.5 (\pm 0.2) \times 10^{-6}$  cm<sup>2</sup>/s, which is in good agreement compared to the accepted literature value of  $7.2 (\pm 0.02) \times 10^{-6}$  cm<sup>2</sup>/s,<sup>44</sup> using the measurements obtained with the commercial instrument. Randles-Sevcik-based measurements of  $D$  for  $[\text{FeCN}_6]^{3-}$  using the home-built PWM- and external DAC-based potentiostats were  $6.2 (\pm 0.7) \times 10^{-6}$  cm<sup>2</sup>/s and  $4.45 (\pm 0.6) \times 10^{-6}$  cm<sup>2</sup>/s respectively.

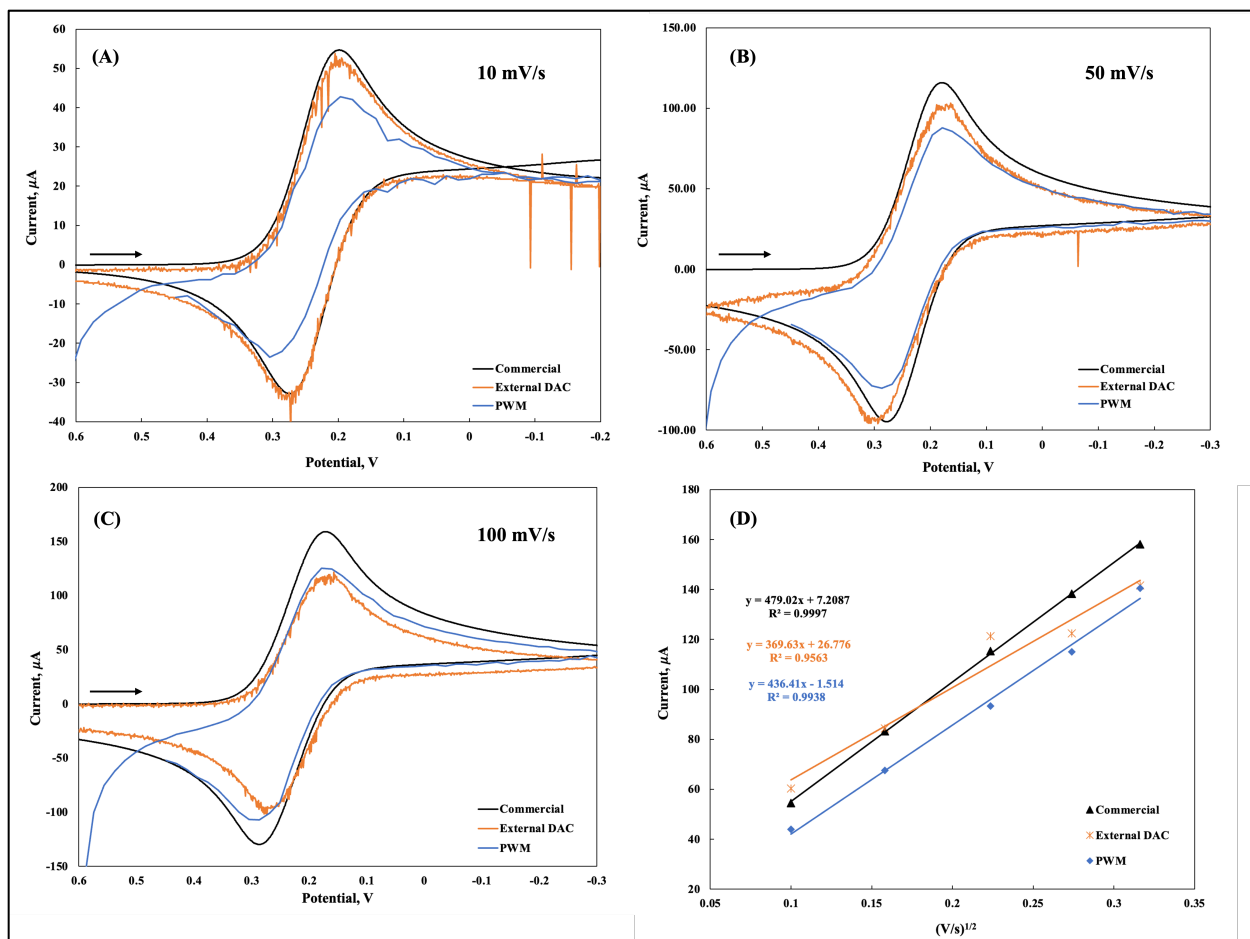


Figure 12. Electrochemical response of 10 mM potassium ferricyanide with 0.1 M KCl supporting electrolyte using home-built and commercial instruments with glassy carbon working electrodes. CVs in at A) 10, B) 50 and C) 100 mV/s. Arrows indicate scan direction. D) Randles-Sevcik plots of CV data.

While the external DAC-based potentiostat showed a close agreement with the commercial instrument at 10 to 50 mV/s, lower currents were recorded at higher scan rates (75 to 100 mV/s). The cause of this result is not clear, but it should be noted that the high rise time (10.3 ms) of the RC filter and the low potential step increment (1.22 mV/step) of the DAC limits the practical upper scan rate<sup>3</sup> of the DAC-based instrument to  $\sim 118$  mV/s.

CV experiments were also performed with a pencil graphite electrode (PGE) (Figure 13) since PGEs are of great interest as platforms for low-cost electrochemical sensors.<sup>41,45</sup> The measured diffusion coefficient ( $D$ ) of ferricyanide obtained from the glassy carbon experiments with the commercial instrument was used to determine the area of the PGE. Based on the scan rate dependence of the ferricyanide peak current using the Randles-Sevcik equation (Equation 14), the area of the PGE was calculated to be  $1.96 (\pm 0.07) \times 10^{-3} \text{ cm}^2$ , which is consistent with the geometric area of the disk-shaped PGE ( $0.00196 \text{ cm}^2$ ) prepared from 0.5 mm diameter pencil graphite.<sup>41</sup>

To effectively measure lower currents associated with PGEs using the home-built potentiostats, the typical  $12 \text{ k}\Omega$  feedback resistor in the current-to-voltage converter was replaced with a  $50 \text{ k}\Omega$  resistor, resulting a full-scale current range of  $\pm 50 \mu\text{A}$  and theoretical current resolution limit of  $\sim 98 \text{ nA}$ . Compared to measurements obtained with the commercial instruments, those obtained with the Arduino potentiostats exhibited larger than expected charging and peak currents. Peaks obtained at lower scan rates were particularly noisy due to the limited current resolution of the ADC and small signal associated with the Faradaic reaction under these conditions. Peaks currents could not even be determined for scans at  $10$  and  $25 \text{ mV/s}$  for the PWM based potentiostat. Overall, slopes for Randles-Sevcik plots for the PGE results obtained with the home-built potentiostats were much larger than those obtained with the commercial instrument, with the slopes for DAC- and PWM-based instruments being more than 7 and 12 times larger, respectively, compared to that obtained with the commercial instrument.

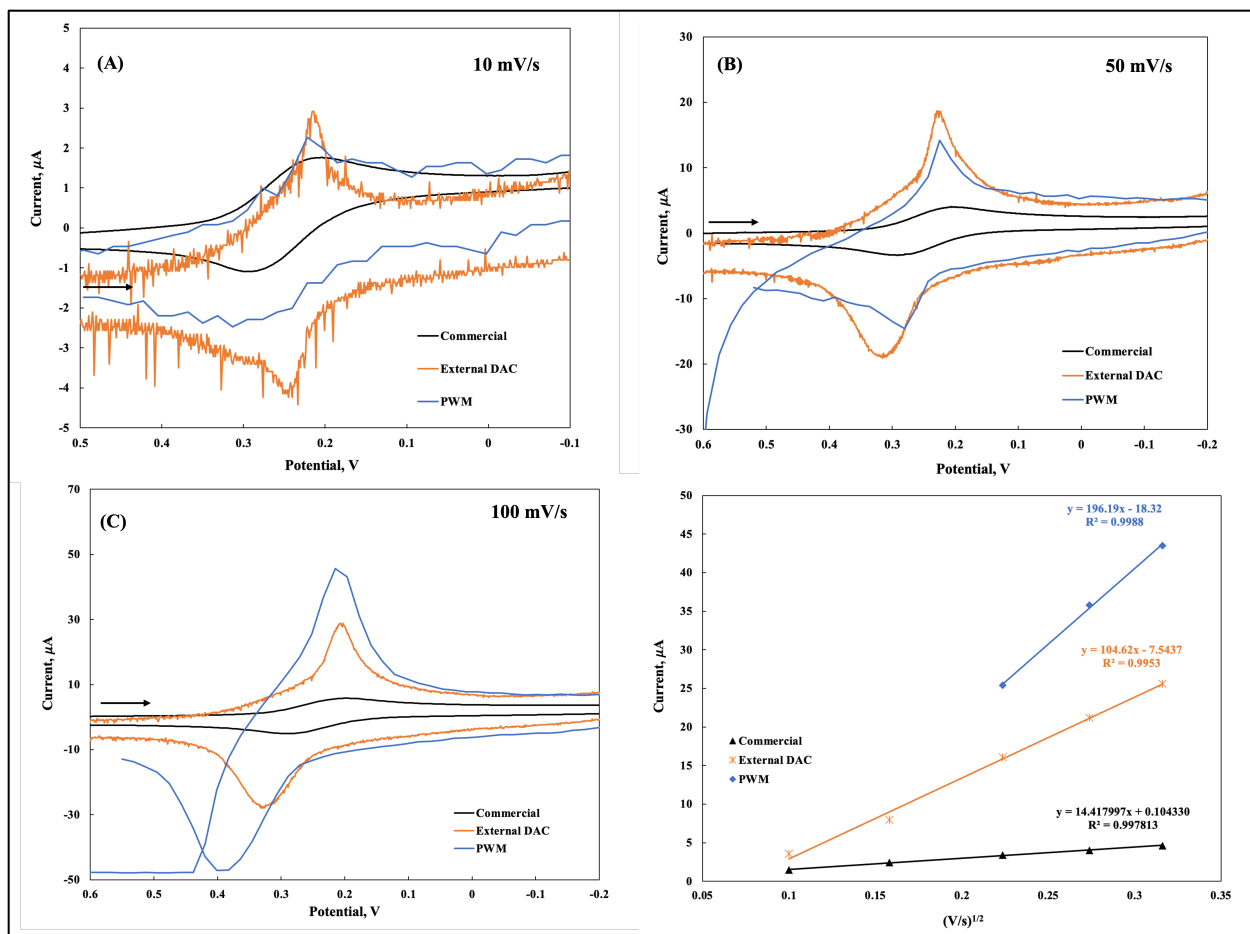


Figure 13. Electrochemical performances of Home-built and Commercial instruments with pencil graphite electrode. A-C) CV in 10 mM potassium ferricyanide with 0.1 M KCl supporting electrolyte at 10 mV/s. Arrows indicates direction of scan. D) Randles-Sevcik plot of peak currents vs. square root of scan rates (V/s)<sup>1/2</sup>.

The source of these discrepancies is not yet known, but it was observed that repeat CV experiments with the commercial instrument after scans with the home-built instruments had been completed yielded much larger currents than those that were obtained in earlier experiments (Figure 14).

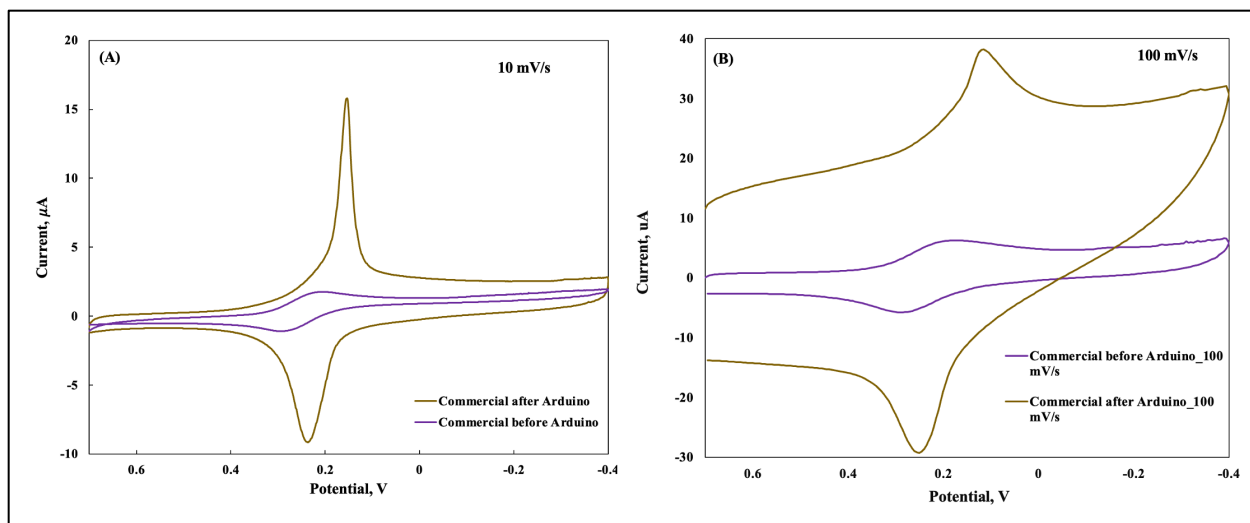


Figure 14. CV response of pencil graphite electrode before and after Arduino scans. A) Commercial instrument response before and after Arduino scans at 10 mV/s. B) Commercial instrument response before and after Arduino scans at 100 mV/s.

## CHAPTER 4. CONCLUSIONS AND FUTURE WORK

Home-built potentiostats based on the open-source Arduino Nano Every microcontroller development board demonstrated good current-voltage relationships comparable to a commercial instrument over the full-scale voltage and current ranges of  $\pm 2.5$  V and  $\pm 200$   $\mu$ A, respectively. Resistor tests with the external DAC version exhibited less variation in (-0.83% to +0.50%) than the PWM version of the potentiostat (0% to 2.6%). Though the external DAC potentiostat exhibited good performance, its high resolution combined with the high rise time of the RC filter employed in the potentiostatic control circuit limits the scan rate of the instrument to less than 118 mV/s while the PWM version gave a noisier response due to the square-wave nature of its source.

CV performances of both home-built potentiostats with the commercial glassy carbon electrode gave the expected peak-shaped response for common redox probe ferricyanide. However, evaluation of the scan rate dependence of CV peak current with the DAC- and PWM-based potentiostats produced calculated diffusion coefficients that were 41% and 18% lower compared to the accepted literature value. It was observed that peak currents obtained with the DAC-based instrument at lower scan rates were more consistent with the commercial instrument while those obtained at higher scan rates were significantly lower. The source of this discrepancy is not yet known but may be due to the stability of the electrode in ferricyanide and/or the high rise time of the RC filter.

CVs with pencil graphite electrodes exhibited more significant differences between the home-built potentiostats and the commercial instrument with larger background charging and peak currents measured using the home-built instruments compared to the commercial one. Interestingly, repeat experiments with the commercial instrument also exhibited larger charging

and peak currents, so more experiments are necessary to determine the source of the unexpected increases.

The current design of the home-built potentiostats utilizes the microcontroller development board USB-derived 5 V power to supply the integrated circuits and as the reference for the PWM and DAC for convenience. Fluctuations in this source voltage can lead to noise in electrochemical measurements. This can be resolved by referencing the DAC, PWM and integrated circuits on both builds to a high precision voltage reference or a low-cost component such as a voltage regulator. The current breadboard version of the home-built instruments can be migrated to a printed circuit board or a perfboard to further reduce noise in measurements. Home-built platforms could also be interfaced with Bluetooth<sup>27,28</sup> (or through the utilization of a microcontroller development board with integrated Bluetooth) for possible application with portable sensors. Further advancements of both DAC and PWM versions can involve the integration with positioning systems like Dropbot developed by Dryden et al. and scanning probe measurements such as the one developed by Meloni and Guver et al.<sup>2,29</sup>

## REFERENCES

- (1) Douglas, A. S.; F. James, H.; Stanley, R. C. Principles of Instrumental Analysis. *Pure and Applied Chemistry*. Cengage Learning 2016, pp 265–291. <https://doi.org/10.1515/pac-2015-0305>.
- (2) Dryden, M. D. M.; Wheeler, A. R. DStat: A Versatile, Open-Source Potentiostat for Electroanalysis and Integration. *PLoS One* **2015**, *10* (10). <https://doi.org/10.1371/journal.pone.0140349>.
- (3) Meloni, G. N. Building a Microcontroller Based Potentiostat: A Inexpensive and Versatile Platform for Teaching Electrochemistry and Instrumentation. *J Chem Educ* **2016**, *93* (7), 1320–1322. <https://doi.org/10.1021/acs.jchemed.5b00961>.
- (4) Resnick, M.; Berg, R.; Eisenberg, M. Beyond Black Boxes: Bringing Transparency and Aesthetics Back to Scientific Investigation. *Journal of the Learning Sciences* **2000**, *9* (1), 7–30. [https://doi.org/10.1207/s15327809jls0901\\_3](https://doi.org/10.1207/s15327809jls0901_3).
- (5) Dryden, M. D. M.; Fobel, R.; Fobel, C.; Wheeler, A. R. Upon the Shoulders of Giants: Open-Source Hardware and Software in Analytical Chemistry. *Anal Chem* **2017**, *89* (8), 4330–4338. <https://doi.org/10.1021/acs.analchem.7b00485>.
- (6) Meloni, G. N. 3D Printed and Microcontrolled: The One Hundred Dollars Scanning Electrochemical Microscope. *Anal Chem* **2017**, *89* (17), 8643–8649. <https://doi.org/10.1021/acs.analchem.7b01764>.
- (7) Davis, E. J.; Jones, M.; Thiel, D. A.; Pauls, S. Using Open-Source, 3D Printable Optical Hardware to Enhance Student Learning in the Instrumental Analysis Laboratory. *J Chem Educ* **2018**, *95* (4), 672–677. <https://doi.org/10.1021/acs.jchemed.7b00480>.
- (8) Rowe, A. A.; Bonham, A. J.; White, R. J.; Zimmer, M. P.; Yadgar, R. J.; Hobza, T. M.; Honea, J. W.; Ben-Yaacov, I.; Plaxco, K. W. Cheapstat: An Open-Source, “Do-It-Yourself” Potentiostat for Analytical and Educational Applications. *PLoS One* **2011**, *6* (9). <https://doi.org/10.1371/journal.pone.0023783>.
- (9) Otal, E. H.; Kim, M. L.; Dietrich, S.; Takada, R.; Nakaya, S.; Kimura, M. Open-Source Portable Device for the Determination of Fluoride in Drinking Water. *ACS Sens* **2021**, *6* (1), 259–266. <https://doi.org/10.1021/acssensors.0c02273>.
- (10) Stoeckli, M.; Staab, D. Reproducible Matrix Deposition for MALDI MSI Based on Open-Source Software and Hardware. *J Am Soc Mass Spectrom* **2015**, *26* (6), 911–914. <https://doi.org/10.1007/s13361-015-1099-9>.
- (11) Szymula, K. P.; Magaraci, M. S.; Patterson, M.; Clark, A.; Mannickarottu, S. G.; Chow, B. Y. An Open-Source Plate Reader. *Biochemistry* **2019**, *58* (6), 468–473. <https://doi.org/10.1021/acs.biochem.8b00952>.

- (12) Jin, H.; Qin, Y.; Pan, S.; Alam, A. U.; Dong, S.; Ghosh, R.; Deen, M. J. Open-Source Low-Cost Wireless Potentiometric Instrument for PH Determination Experiments. *J Chem Educ* **2018**, *95* (2), 326–330. <https://doi.org/10.1021/acs.jchemed.7b00479>.
- (13) Grinias, J. P.; Whitfield, J. T.; Guetschow, E. D.; Kennedy, R. T. An Inexpensive, Open-Source USB Arduino Data Acquisition Device for Chemical Instrumentation. *J Chem Educ* **2016**, *93* (7), 1316–1319. <https://doi.org/10.1021/acs.jchemed.6b00262>.
- (14) Otal, E. H.; Kim, M. L.; Dietrich, S.; Takada, R.; Nakaya, S.; Kimura, M. Open-Source Portable Device for the Determination of Fluoride in Drinking Water. *ACS Sens* **2021**, *6* (1), 259–266. <https://doi.org/10.1021/acssensors.0c02273>.
- (15) Harnett, C. *Open Source Hardware for Instrumentation and Measurement*. <http://www.thingiverse.com/thing:5045>.
- (16) Fisher, D. K.; Gould, P. J. Open-Source Hardware Is a Low-Cost Alternative for Scientific Instrumentation and Research. *Modern Instrumentation* **2012**, *01* (02), 8–20. <https://doi.org/10.4236/mi.2012.12002>.
- (17) IEEE Staff; IEEE Staff. *2012 IEEE International Instrumentation and Measurement Technology Conference*.
- (18) *Bitbucket*. <https://bitbucket.org>. (accessed June 29, 2023)
- (19) *Github: Where open source lives*. <https://github.com/open-source>. (accessed June 29, 2023).
- (20) *GitLab*. <https://about.gitlab.com>. (accessed June 29, 2023).
- (21) *Top Open Source Licenses*. <https://www.blackducksoftware.com/top-open-source-licenses>. (accessed June 29, 2023).
- (22) Urban, P. L. Open-Source Electronics as a Technological Aid in Chemical Education. *J Chem Educ* **2014**, *91* (5), 751–752. <https://doi.org/10.1021/ed4009073>.
- (23) Institute of Electrical and Electronics Engineers; IEEE Computer Society; American Society for Engineering Education. *Frontiers in Education 2015 : Launching a New Vision in Engineering Education : Proceedings : October 21-24, 2015, Camino Real Hotel & Conference Center, El Paso, Texas*.
- (24) Munafò, M. R.; Nosek, B. A.; Bishop, D. V. M.; Button, K. S.; Chambers, C. D.; Percie Du Sert, N.; Simonsohn, U.; Wagenmakers, E. J.; Ware, J. J.; Ioannidis, J. P. A. A Manifesto for Reproducible Science. *Nature Human Behaviour*. Nature Publishing Group January 10, 2017. <https://doi.org/10.1038/s41562-016-0021>.
- (25) Pearce, J. M. *Open-Source Lab: How to Build Your Own Hardware and Reduce Research Costs*; Elsevier, 2013.

- (26) Jeong, H.; Shin, S.; Hwang, J.; Kim, Y. J.; Choi, S. Open-Source Fluorescence Spectrometer for Noncontact Scientific Research and Education. *J Chem Educ* **2021**, *98* (11), 3493–3501. <https://doi.org/10.1021/acs.jchemed.1c00560>.
- (27) Cordova-Huaman, A. V.; Jauja-Ccana, V. R.; La Rosa-Toro, A. Low-Cost Smartphone-Controlled Potentiostat Based on Arduino for Teaching Electrochemistry Fundamentals and Applications. *Heliyon* **2021**, *7* (2). <https://doi.org/10.1016/j.heliyon.2021.e06259>.
- (28) Ainla, A.; Mousavi, M. P. S.; Tsaloglou, M. N.; Redston, J.; Bell, J. G.; Fernández-Abedul, M. T.; Whitesides, G. M. Open-Source Potentiostat for Wireless Electrochemical Detection with Smartphones. *Anal Chem* **2018**, *90* (10), 6240–6246. <https://doi.org/10.1021/acs.analchem.8b00850>.
- (29) Guver, A.; Fifita, N.; Milas, P.; Straker, M.; Guy, M.; Green, K.; Yildirim, T.; Unlu, I.; Yigit, M. V.; Ozturk, B. A Low-Cost and High-Precision Scanning Electrochemical Microscope Built with Open Source Tools. *HardwareX* **2019**, *6*. <https://doi.org/10.1016/j.ohx.2019.e00082>.
- (30) Colburn, A. W.; Levey, K. J.; O'Hare, D.; Macpherson, J. V. Lifting the Lid on the Potentiostat: A Beginner's Guide to Understanding Electrochemical Circuitry and Practical Operation. *Physical Chemistry Chemical Physics*. Royal Society of Chemistry April 14, 2021, pp 8100–8117. <https://doi.org/10.1039/d1cp00661d>.
- (31) Bard, A. J.; Faulkner, L. R. *Electrochemical Methods : Fundamentals and Applications*, 2nd ed.; Annu. Rev. Mater. Sci, 2000; Vol. 2.
- (32) Nemiroski, A.; Christodouleas, D. C.; Hennek, J. W.; Kumar, A. A.; Maxwell, E. J.; Fernández-Abedul, M. T.; Whitesides, G. M. Universal Mobile Electrochemical Detector Designed for Use in Resource-Limited Applications. *Proc Natl Acad Sci U S A* **2014**, *111* (33), 11984–11989. <https://doi.org/10.1073/pnas.1405679111>.
- (33) Dobbelaere, T.; Vereecken, P. M.; Detavernier, C. A USB-Controlled Potentiostat/Galvanostat for Thin-Film Battery Characterization. *HardwareX* **2017**, *2*, 34–49. <https://doi.org/10.1016/j.ohx.2017.08.001>.
- (34) Li, Y. C.; Melenbrink, E. L.; Cordonier, G. J.; Boggs, C.; Khan, A.; Isaac, M. K.; Nkhonjera, L. K.; Bahati, D.; Billinge, S. J.; Haile, S. M.; Kreuter, R. A.; Crable, R. M.; Mallouk, T. E. An Easily Fabricated Low-Cost Potentiostat Coupled with User-Friendly Software for Introducing Students to Electrochemical Reactions and Electroanalytical Techniques. *J Chem Educ* **2018**, *95* (9), 1658–1661. <https://doi.org/10.1021/acs.jchemed.8b00340>.
- (35) Jenkins, D. M.; Lee, B. E.; Jun, S.; Reyes-De-Corcuera, J.; McLamore, E. S. ABE-Stat, a Fully Open-Source and Versatile Wireless Potentiostat Project Including Electrochemical Impedance Spectroscopy. *J Electrochem Soc* **2019**, *166* (9), B3056–B3065. <https://doi.org/10.1149/2.0061909jes>.

- (36) Glasscott, M. W.; Verber, M. D.; Hall, J.; Pendergast, A. D.; Mckinney, C. J.; Dick, J. E. *SweepStat: A Build-It-Yourself, Two-Electrode Potentiostat for Macroelectrode and Ultramicroelectrode Studies*.
- (37) *Arduino Uno Rev 3*. <https://store-usa.arduino.cc/products/arduino-uno-rev3?selectedStore=us>. (accessed July 2, 2023).
- (38) *DigiKey Electronics*. <https://www.digikey.com/en/products/detail/microchip-technology/ATXMEGA256A3U-MHR/3678724>. (accessed June 27, 2023).
- (39) Erkal, J. L.; Selimovic, A.; Gross, B. C.; Lockwood, S. Y.; Walton, E. L.; McNamara, S.; Martin, R. S.; Spence, D. M. 3D Printed Microfluidic Devices with Integrated Versatile and Reusable Electrodes. *Lab Chip* **2014**, *14* (12), 2023–2032. <https://doi.org/10.1039/c4lc00171k>.
- (40) Bishop, G. W.; Satterwhite-Warden, J. E.; Bist, I.; Chen, E.; Rusling, J. F. Electrochemiluminescence at Bare and DNA-Coated Graphite Electrodes in 3D-Printed Fluidic Devices. *ACS Sens* **2016**, *1* (2), 197–202. <https://doi.org/10.1021/acssensors.5b00156>.
- (41) Antwi, I. An Electrochemical Immunoassay System for Measuring Circulating Protein Biomarkers of Pediatric Soft Tissue Sarcoma. Master's Thesis, East Tennessee State University, Tennessee, U.S.A., 2021.
- (42) Aristov, N.; Habekost, A. Cyclic Voltammetry-A Versatile Electrochemical Method Investigating Electron Transfer Processes. *World Journal of Chemical Education* **2015**, *3* (5), 115–119. doi: 10.12691/wjce-3-5-2.
- (43) Hendel, S. J.; Young, E. R. Introduction to Electrochemistry and the Use of Electrochemistry to Synthesize and Evaluate Catalysts for Water Oxidation and Reduction. *J Chem Educ* **2016**, *93* (11), 1951–1956. <https://doi.org/10.1021/acs.jchemed.6b00230>.
- (44) Konopka, S. J.; McDuffie, B.; Arvia, A. J.; Bazan, J. C.; W Carrozza, J. S. *Polarographic Techniques*; 1929; Vol. 10. <https://pubs.acs.org/sharingguidelines>.
- (45) Chikkaveeraiah, B. V.; Mani, V.; Patel, V.; Gutkind, J. S.; Rusling, J. F. Microfluidic Electrochemical Immunoarray for Ultrasensitive Detection of Two Cancer Biomarker Proteins in Serum. *Biosens Bioelectron* **2011**, *26* (11), 4477–4483. <https://doi.org/10.1016/j.bios.2011.05.005>.

## APPENDICES

### Appendix A: Arduino Sketch for PWM Potentiostat

```
//Script starts

//User defines parameters for experiment
int const rate = 50 //for setting scan rate in mV/s (max 118 mV/s)
int Estart = 600; //for setting starting potential between +/- 2500 mV
int Eswitch = -400; //for setting switching potential between +/- 2500 mV
int Eend = 600; //for setting end potential between +/- 2500 mV

float m = 0; // variable to define slope for current conversion, current range (-2.5V/R4 to -
(5V+2.5V)/R4) div 0 to 1023 ADC levels
float b = 208; // variable to define y-int for current conversion
int res = 1; // variable to define resolution for current conversion
int dac = 6; // define pin for digital-to-analog converter output
int PWMval = 0; // variable for setting PWM value
int ct = A0; // define pin for analog-to-digital current input
int ap = 7; // define pin +5V supply to op amp LMC6484/OPA340PA
float i = 0; // variable to store current
float Potstep = 19.608; // Voltage range -2500 to +2500 mV divided by 0 to 255 PWM levels
int const count = 1; // set number of sweep cycles
int n = 0; // counter for sweep cycle repeats

void setup() {
  // set dividers to change PWM frequency on pin 6
  TCB0_CTRLA = (TCB_CLKSEL_CLKDIV2_gc) | (TCB_ENABLE_bm);
  //Set baud
  Serial.begin(9600);
  // set output pin for opamps LMC6484/OPA340PA
  pinMode(dac,OUTPUT);
  // set input pin for ADC current
  pinMode(ap,OUTPUT);
  // set output pin for DAC voltage
  pinMode(ct,INPUT);
  // time delay
  delay(2500);
  // positive supply to op amp LMC6484/OPA340PA (high)
  digitalWrite(ap,1);
  // time delay
  delay(3000);
  Serial.print("Rate:");
  Serial.print(rate);
  Serial.print("mV/s");
}
```

```

Serial.print(" ");
//variable to define slope for current conversion, current range (-2.5V/R4 to -(5V+2.5V)/R4) div
0 to 1023 ADC levels;
{ m = -0.4066;// defines the slope of current measurement
  b = 208;//defines the intercept of current measurement
  res = 1;//defines the level of precision
}
Serial.print("PWMval");
Serial.print(" ");
Serial.print("mV");
Serial.print(" ");
Serial.print("uA");
Serial.print(" ");
Serial.println("A0val");
// force potentials to range determined by potentiostatic control circuit
if(Estart < -2500){
  Estart = -2500;
}
if(Estart > 2500){
  Estart = 2500;
}
if(Eswitch < -2500){
  Eswitch = -2500;
}
if(Eswitch > 2500){
  Eswitch = 2500;
}
if(Eend < -2500){
  Eend = -2500;
}
if(Eend > 2500){
  Eend = 2500;
}
delay(100);
}

void loop () {
  while(n < count){
    if(Estart <= Eswitch){// determine whether scan direction is positive or negative
      for(PWMval = 255+(Estart-2500)/Potstep; PWMval <= 255+(Eswitch-2500)/Potstep;
PWMval++){
        analogWrite(dac,PWMval); // changes PWM level at DAC output
        Serial.print(PWMval); // prints PWM level
        Serial.print(" ");
        Serial.print(Potstep*(PWMval-255)+2500,1); // prints PWM in terms of voltage
      }
    }
  }
}

```

```

    delay(1000000L/(rate*51L)); // waits to read current and change PWM level (V) based on
scan rate
    i=((m*analogRead(ct))+b); //output current in uA
    Serial.print(" ");
    Serial.print(i,res);
    Serial.print(" ");
    Serial.println(analogRead(ct));
    n=n+1;
    }}
    else { // in case scan direction is negative
        for(PWMval = 255+(Estart-2500)/Potstep; PWMval >= 255+(Eswitch-2500)/Potstep;
PWMval--){
            analogWrite(dac,PWMval); // changes PWM level at DAC output
            Serial.print(PWMval); // prints PWM level
            Serial.print(" ");
            Serial.print(Potstep*(PWMval-255)+2500,1); // prints PWM in terms of voltage
            delay(1000000L/(rate*51L)); // waits to read current and change PWM level (V) based on
scan rate ms/step = (1000 mV/V*1000 ms/s)/(Rate mV/s*255 PWM step/(5 V range))
            i=((m*analogRead(ct))+b); //output current in uA
            Serial.print(" ");
            Serial.print(i,res);
            Serial.print(" ");
            Serial.println(analogRead(ct));
            n=n+1;
            }}
        if(Eswitch >= Eend){
            for(PWMval = 255+(Eswitch-2500)/Potstep; PWMval >= 255+(Eend-2500)/Potstep;
PWMval--){
                analogWrite(dac,PWMval);
                Serial.print(PWMval);
                Serial.print(" ");
                Serial.print(Potstep*(PWMval-255)+2500,1);
                delay(1000000L/(rate*51L));
                i=((m*analogRead(ct))+b);
                Serial.print(" ");
                Serial.print(i,res);
                Serial.print(" ");
                Serial.println(analogRead(ct));
                n=n+1;
                }}
            else{
                for(PWMval = 255+(Eswitch-2500)/Potstep; PWMval <= 255+(Eend-2500)/Potstep;
PWMval++){
                    analogWrite(dac,PWMval);
                    Serial.print(PWMval);
                    Serial.print(" ");

```

```
Serial.print(Potstep*(PWMval-255)+2500,1);  
delay(1000000L/(rate*51L));  
i=((m*analogRead(ct))+b);  
Serial.print(" ");  
Serial.print(i,res);  
Serial.print(" ");  
Serial.println(analogRead(ct));  
n=n+1;  
}}  
}  
delay(100);  
}  
  
// Script Ends
```

## Appendix B: Arduino Sketch for External DAC

```
//Script starts

//User defines defines parameters for experiment.

int const rate = 100; //for setting scan rate in mV/s (max 118 mV/s)
int Estart = 2280; //for setting starting potential between +/- 2500 mV
int Eswitch = -2280; //for setting switching potential between +/- 2500 mV
int Eend = -2280; //for setting end potential between +/- 2500 mV

#include <Wire.h>
#include <Adafruit_MCP4725.h>
Adafruit_MCP4725 dac;
float m = 0; // variable to define slope for current conversion, current range (-2.5V/R5 to(-
(5V+2.5V)/R5) div 0 to 1023 ADC levels
float b = 0; // variable to define y-int for current conversion
int res = 0; // variable to define resolution for current conversion
int DACval = 0; // variable for setting DAC value
int ct = A0; // define pin for analog-to-digital current input
int op = 7; // define pin +5V supply to op amp OPA344PA
int lm = 8; //define pin +5 supply to op amp LMC6484IN
float i = 0; // variable to store current
float Potstep = 1.22; // Voltage range -2500 to +2500 mV divided by 0 to 4095 DAC levels
int const count = 1; // set number of sweep cycles
int n = 0; // counter for sweep cycle repeats

void setup() {
  //Set baud
  Serial.begin(9600);
  dac.begin (0x60);
  // set output pin for opamp LMC6484IN
  pinMode (lm, OUTPUT);
  // set output pin for opamp OPA340PA
  pinMode (op, OUTPUT);
  // set input pin for ADC voltage
  pinMode(ct,INPUT);
  // time delay
  delay(2500);
  // positive supply to opamp OPA340PA (high)
  digitalWrite(op,1);
  //positive supply to opamp LMC6484IN (high)
  digitalWrite (lm,1);
  // time delay
  delay(3000);
  Serial.print("Rate:");
```

```

Serial.print(rate);
Serial.print("mV/s");
Serial.print(" ");
//variable to define slope for current conversion, current range (-2.5V/R5 to(-(5V+2.5V)/R5) div
0 to 1023 ADC levels);
{
  m = -0.4073;// defines the slope of current measurement
  b = 208; // defines the intercept of current measurement
  res = 1;// defines the level of precision
}
Serial.print("DACval");
Serial.print(" ");
Serial.print("mV");
Serial.print(" ");
Serial.print("uA");
Serial.print(" ");
Serial.println("A0val");
// force potentials to range determined by potentiostatic control circuit
if(Estart < -2280){
  Estart = -2280.;
}
if(Estart > 2280){
  Estart = 2280;
}
if(Eswitch < -2280){
  Eswitch = -2280;
}
if(Eswitch > 2280){
  Eswitch = 2280;
}
if(Eend < -2280){
  Eend = -2280;
}
if(Eend > 2280){
  Eend = 2280;
}
delay(100);
DACval = 4095 + (Estart-2280);
Dac.setVoltage (DACval, false);
delay(2000);
}

void loop () {
  dac.setVoltage (4095, false);// This is a mistake and should be removed in future experiments
  while(n < count){
    if(Estart <= Eswitch){// determine whether scan direction is positive or negative

```



```

else{
  for(DACval = 4095+(Eswitch-2280)/Potstep; DACval <= 4095+(Eend-2280)/Potstep;
DACval++){
  dac.setVoltage (DACval,false);
  Serial.print(DACval);
  Serial.print(" ");
  Serial.print(Potstep*(DACval-4095)+2280,1);
  delay(1000000L/(rate*898L));
  i=((m*analogRead(ct))+b);
  Serial.print(" ");
  Serial.print(i,res);
  Serial.print(" ");
  Serial.println(analogRead(ct));
  n=n+1;
  }}
}
delay(100);
}
// Script Ends

```

## VITA

MICHAEL KOFI DARKO ADDO

- Education: B.Sc. Chemistry, Kwame Nkrumah University of Science and Technology, Kumasi, Ghana, 2017  
M.S. Chemistry, East Tennessee State University, Johnson City, Tennessee, 2023
- Professional Experience: Medical Laboratory Scientist, Tafo Government Hospital, Kumasi, Ghana, August 2017 – July 2018  
Chemistry Teacher, Ghana Education Service, Tarkwa, Ghana, November 2018 – July 2021  
Graduate Assistant, East Tennessee State University, College of Arts and Sciences, August 2021 – May 2023
- Honors and Awards: The Miss Margaret Sells Chemistry Scholarship for Outstanding Graduate Students in Chemistry, East Tennessee State University, Johnson City, TN April – 29 – 2023
- Presentations: M. Addo, Ivy Antwi and Gregory Bishop, An Electrochemical Immunoassay System for Measuring Circulating Protein Biomarkers of Pediatric Soft Tissue Sarcoma.  
Poster Presentation at the 242<sup>nd</sup> Electrochemical Society (ECS) Meeting, Atlanta, October 2022.  
M. Addo, Ivy Antwi and Gregory Bishop, An Electrochemical Immunoassay System for Measuring Circulating Protein Biomarkers of Pediatric Soft Tissue Sarcoma.

3 Minutes Thesis (3MT<sup>®</sup>) Presentation, East Tennessee State  
University, November 2022.

M. Addo and Gregory Bishop, A Low Cost, Compact  
Electrochemical Analyzer based on an Open-Source  
Microcontroller.

Poster Presentation at the Appalachian Student Research Forum,  
East Tennessee State University, April 2023.